J. Vis. Commun. Image R. 112 (2025) 104572

Contents lists available at ScienceDirect

J. Vis. Commun. Image R.

journal homepage: www.elsevier.com/locate/jvci

Review

Survey: 3D watermarking techniques☆

Ertugrul Gul [a,b], Gary K.L. Tam [a,*]

[a] Department of Computer Science, Swansea University, Swansea, United Kingdom
[b] Department of Software Engineering, Kayseri University, Kayseri, Turkey

ARTICLE INFO

Keywords:
3D watermarking
3D image/video
3D mesh/point cloud
NeRF

ABSTRACT

In today's world, 3D multimedia data is widely utilized in diverse fields such as military, medical, and remote sensing. The advancement of multimedia technologies, however, exposes 3D multimedia content to an increasing risk of malicious interventions. It has become highly essential to implement security measures ensuring the authenticity and copyright protection of 3D multimedia content. Watermarking is considered one of the most reliable and practical approaches for this purpose. This work provides an in-depth and up-to-date overview of various 3D watermarking methods, covering different data forms, including 3D images, 3D videos, 3D meshes, point clouds, and NeRF. We have categorized these methods from multiple perspectives, comparing their respective advantages and disadvantages. The study also identifies attacks based on data type and discusses metrics for evaluating the methods according to their intended use and data type. We further present observations, research issues, challenges, and future directions for 3D watermarking. This includes strength factor optimization, copyright concerns related to 3D printed objects, detection and recovery of tampered areas, and watermarking in 4D (3D Dynamic) and NeRF domains.

Contents

☆ This paper has been recommended for acceptance by Zicheng Liu.

* Corresponding author.
E-mail address: k.l.tam@swansea.ac.uk (G.K.L. Tam).

https://doi.org/10.1016/j.jvcir.2025.104572
Received 16 December 2024; Received in revised form 25 July 2025; Accepted 19 August 2025
Available online 27 August 2025

1. Introduction

With rapid advances in signal processing and the widespread use of the internet and multimedia technologies, the sharing of multimedia data (images, videos, and audio) has surged significantly [1]. This increased accessibility, however, introduces risks like intentional or unintentional interventions, attacks, manipulations, deformations, unauthorized access, and even illegal claims of ownership [2]. Protecting digital multimedia data is more crucial than ever before, and watermarking emerges as a highly effective method to address these challenges.

Watermarking is a process that embeds a digital code, known as a watermark, into multimedia content (the cover data) such as text [3,4], audio [5,6], images [7–9], and video [10,11]. By incorporating a unique watermark into multimedia data, creators can ensure their work is easily identifiable and traceable. Watermarking methods find applications in various areas [12–14], including military [15], medical [16], broadcasting [17], remote sensing [18], and communication [19]. In these domains, watermarking serves purposes such as authentication [20], copyright protection [21–23], traitor tracing [24,25], broadcast monitoring [26], copy or playback control [27], content filtering [28], and tamper detection [29,30]. Watermarking plays a vital role in ensuring data security.

With the recent advances in 3D sensing technology and 3D modeling tools, the use of 3D shapes has surged in fields like video games, medical diagnostics, computer-aided design, virtual reality, 3D modeling, and 3D printing. Protecting the intellectual property of these 3D content has become paramount for commercial investment and creativity efforts. Compared to traditional 2D image and 1D signal (e.g., audio) watermarking, 3D watermarking is a comparatively new and rapidly developing field. This survey aims to provide a comprehensive survey of contemporary 3D watermarking techniques and to drive ongoing research efforts for the community.

Existing surveys on 3D watermarking [12,31–35] typically focus on specific data types like 3D mesh, image, or video watermarking. For example, [31,34], and [35] exclusively explore 3D mesh watermarking, while [12] delves into 3D video watermarking. [32] centers on 3D image and point cloud watermarking, and [33] focuses on 3D image and video watermarking. Our survey, in contrast, aims to comprehensively cover all 3D watermarking methods, encompassing 3D image, 3D video, 3D mesh, and point cloud. Notably, our survey includes Neural Radiance Field (NeRF) [36], which has garnered attention in recent years for its potential to generate novel views of complex 3D scenes from a partial set of 2D images. Table 1 compares ours with existing surveys. We classify methods based on embedding domains and data types, discuss the drawbacks and advantages of methods, gather and categorize evaluation metrics for 3D watermarking techniques, and explore challenges and future research directions in the field.

The main contributions of this survey can be summarized as follows.

- In contrast to other surveys that concentrate on specific types of data, our survey comprehensively covers various 3D watermarking methods, including 3D images, 3D videos, 3D meshes, and point clouds. We also include NeRF and 4D watermarking, which hold immense potential and can be the future direction of the watermarking research.
- We classify 3D watermarking methods according to distortion, robustness, and data type. We also survey and classify watermarking methods based on the technical properties for a more in-depth discussion. Moreover, we also provided an analysis of the drawbacks and advantages of the 3D watermarking methods.

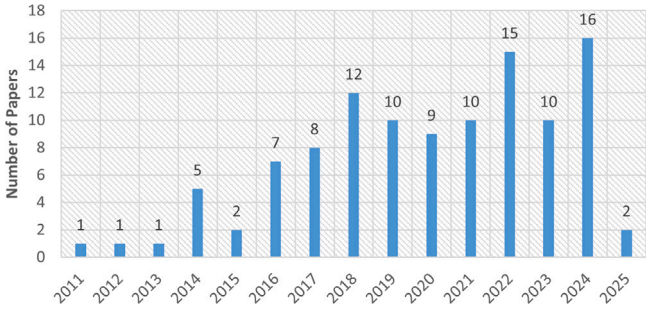

Fig. 1. Reviewed paper statistics.

- We survey commonly used datasets in the field and evaluation metrics based on their purpose and the data type.
- Challenges in 3D watermarking are discussed, including issues such as robustness against print-scan attacks and the delicate balance between robustness and imperceptibility. We also delved into the future research direction of watermarking, encompassing areas like dynamic 3D mesh watermarking, deep learning-based watermarking, and NeRF.

We observed that while certain techniques are commonly used within one media type, they may not be recognized or applied in others. By analyzing these differences, our study explores the underlying reasons and potential opportunities for cross-media adaptation, fostering new discoveries and supporting future advancements in watermarking techniques.

The survey is structured as follows. Section 2 outlines the scope of our survey, while Section 3 introduces watermarking background. Section 4 details 3D watermarking attacks, and Section 5 classifies algorithms for distortion. Section 6 surveys and classify methods based on the respective technical properties. Section 7 categorizes algorithms for robustness, and Section 8 discusses input–output differences in some special cases. Section 9 mentions 3D datasets. Evaluation metrics are covered in Section 10. Discussions and future directions are in Section 11. We conclude in Section 12.

2. Scope

Our survey covers a range of 3D watermarking methods tailored for diverse data types, including 3D images, 3D videos, 3D meshes, point clouds, NeRF, and 4D datasets. We conducted a review of recent works published over the past decade until March 21, 2025. The distribution of reviewed papers by year is shown in the bar chart in Fig. 1. For older techniques and papers, readers are directed to relevant surveys [12,31–35]. The literature search utilized the following keywords: “3D watermarking”, “3D video watermarking”, “3D image watermarking”, “3D mesh watermarking”, and “NeRF watermarking”. These keywords were searched across various repositories, including Google Scholar, IEEE Xplore, ScienceDirect, Springer, ACM digital portals, MDPI, Wiley, and arXiv.

3. Background of watermarking

Digital watermarking is the process of embedding information, such as an image, logo, or bit sequence, into the content of multimedia data by the content owner or authorized distributor [37]. The digital watermarking process involves two primary steps: watermark embedding and

Table 1
Comparison to other surveys

Surveys	Year	3D image	3D video	3D mesh	Point cloud	NeRF	Focus
[31]	2022			✓			3D mesh watermarking.
[32]	2022	✓			✓		geometric invariant techniques and emerging watermarking methods for depth image-based rendering (DIBR), high dynamic range (HDR), screen content images (SCIs), and point cloud model.
[33]	2019	✓	✓				anaglyph 3D images and videos watermarking techniques.
[12]	2017		✓				digital watermarking techniques for both 2D and 3D video contents.
[34]	2018			✓			authentication based watermarking techniques for 3D mesh models.
[35]	2018			✓			intellectual property protection problems and solutions for 3D printing environments.
Ours	2025	✓	✓	✓	✓	✓	3D image, 3D video, 3D mesh, point cloud and NeRF watermarking.

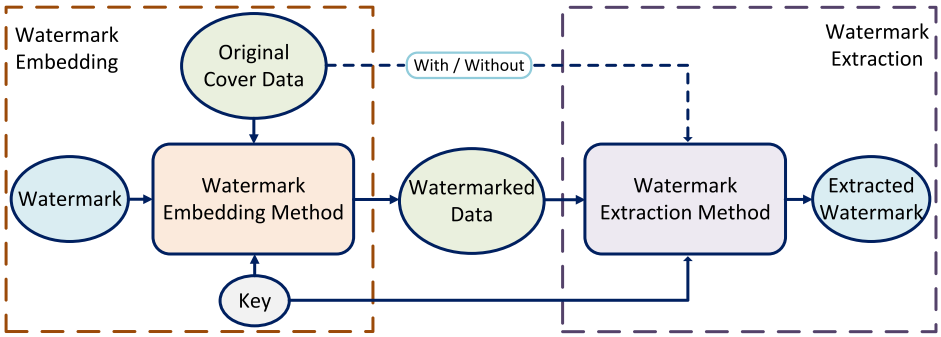

Fig. 2. The watermark embedding and extraction steps.

watermark extraction. In the embedding step, the watermark is inserted into the cover data using various methods, including the least significant bit (LSB), most significant bit (MSB), discrete wavelet transform (DWT), discrete cosine transform (DCT), etc. In the extraction step, the watermark is retrieved from the watermarked data by generally reversing the steps in the embedding process. In the watermarking process, a secret key can be utilized to embed and extract the watermark from digital content, enhancing security by ensuring that only authorized parties can verify the watermark. Fig. 2 demonstrates the watermark embedding and extraction process.

3.1. Watermarking properties

Watermarking methods possess three primary properties: imperceptibility, robustness, and capacity. **Imperceptibility** ensures that the distortion introduced by the watermarking process in the original data remains imperceptible to the human perception system, reflecting the quality of the watermarked data. High imperceptibility is particularly crucial in fields like medicine and defense, where the integrity of the cover data is of utmost importance. **Robustness** indicates the ability of a method to withstand attacks, ensuring the persistence of the watermark in the data for successful extraction. Robust watermarking methods, exhibiting high resistance to attacks, are ideal for applications prone to intentional or unintentional data manipulation, such as digital forensics or copyright protection for online multimedia content. In contrast, fragile watermarking methods are designed for scenarios demanding the detection of minimal tampering. It finds utility in contexts like legal or authentication processes that requires the integrity and authenticity of sensitive documents. **Capacity** refers to the payload of the method. It indicates the maximum size of the embedded watermark. In this context, a higher capacity is generally considered preferable. Each watermarking algorithm is expected to demonstrate these three properties, tailoring to the specific requirements of the application area.

3.2. Classification of properties

Watermarking methods have been classified in various ways based on their characteristics in past surveys. Watermarking algorithms can be categorized as visible or invisible, depending on their visibility to human perception. They can also be classified as blind, semi-blind, or non-blind, based on whether the method requires the original cover data during watermark extraction. In blind watermarking, the watermarking process does not require the original cover data. However, non-blind watermarking requires the original data to extract the watermark, while semi-blind watermarking uses certain features of the original data or the original watermark to extract the watermark. Additionally, algorithms are categorized as robust, semi-fragile, or fragile, according to their resistance to attacks. In fragile watermarking methods, the watermark is expected to collapse against attacks, while in robust watermarking methods, it is expected to maintain its existence. On the other hand, in semi-fragile watermarking methods, the watermark is expected to be robust against attacks determined according to the application area and fragile against different attacks. Watermarking algorithms can also be classified according to the cover data, namely image, video, text, audio, and 3D mesh watermarking [31]. As our survey covers multiple types of inputs, we follow this basic classification strategy and further classify techniques based on specific criteria in subsequent sections (attacks, distortion, robustness etc.).

3.3. Brief reviews of mathematical tools for watermarking

This subsection presents information about mathematical tools, including DCT, DWT, Singular Value Decomposition (SVD), LSB, MSB, normalization, and spherical coordinates, utilized in 3D watermarking algorithms. DCT, DWT, and SVD are preferred for watermarking because they offer enhanced imperceptibility and robustness. In contrast, LSB and MSB are often chosen for their simplicity, though they tend to

be more fragile. Additionally, these algorithms are frequently used in combination to achieve greater success. On the other hand, spherical coordinates and normalization techniques are frequently employed in 3D mesh watermarking, as they enhance the algorithms' resilience to content-preserving attacks.

DCT: Discrete Cosine Transform is among the most commonly utilized transforms for watermarking purposes. The definition of the two-dimensional Discrete Cosine Transform for a given size of $M \times N$ can be articulated using equation (1) as follows [38]:

$$F(u,v) = \frac{2}{\sqrt{MN}} C(u)C(v) \sum_{i=0}^{M-1} \sum_{j=0}^{N-1} f(i,j) cos\left[\frac{(2j+1)v\pi}{2N}\right] cos\left[\frac{(2i+1)u\pi}{2M}\right] \tag{1}$$

here, $v = 0, 1, \ldots, N-1$, $u = 0, 1, \ldots, M-1$, $C(u)$ and $C(v)$ are as in Eq. (2):

$$C(u) = C(v) = \begin{cases} \frac{1}{\sqrt{2}}, & \text{if } u, v = 0 \\ 1, & \text{otherwise} \end{cases} \tag{2}$$

The first coefficient $F(0,0)$ is referred to as the DC coefficient, while the other coefficients are referred to as AC coefficients [38]. Adjusting mid-frequency DC coefficients serves to achieve a balance between robustness and imperceptibility.

DWT: The 2D Discrete Wavelet Transform (DWT) is widely used in image processing and watermarking. It decomposes an image $I(a,b)$ using low-pass $g(n)$ and high-pass $h(n)$ filters, as given in Eqs. (3)–(5). First, DWT is applied along rows:

$$I_L(a,b) = \sum_n I(a,n)g(n), \quad I_H(a,b) = \sum_n I(a,n)h(n) \tag{3}$$

Then, along columns:

$$LL1(a,b) = \sum_m I_L(m,b)g(m), \quad LH1(a,b) = \sum_m I_L(m,b)h(m) \tag{4}$$

$$HL1(a,b) = \sum_m I_H(m,b)g(m), \quad HH1(a,b) = \sum_m I_H(m,b)h(m) \tag{5}$$

satisfying: $I(a,b) = LL1 + LH1 + HL1 + HH1$ where $LL1$ is the low-frequency approximation, while $LH1$, $HL1$, and $HH1$ capture horizontal, vertical, and diagonal details. For watermarking, embedding in $LL1$ ensures robustness, while $LH1$, $HL1$, and $HH1$ maintain imperceptibility.

SVD: Singular Value Decomposition is a linear algebra tool that diagonalizes and decomposes a matrix into eigenvectors and eigenvalues. SVD of a matrix can be expressed in Eq. (6) as follows [39]:

$$A = U \Sigma V^T \tag{6}$$

here, Σ denotes the diagonal matrix containing the singular values of A in decreasing order, while V and U denote the right and left singular vectors, respectively. Singular values can effectively represent much of the signal energy, making watermark extraction efficient and preserving high quality despite various attacks.

LSB and MSB: LSB refers to the lowest bit in a binary sequence, whereas MSB signifies the highest bit in the same sequence [40]. The value of an N-bit number can typically be represented as demonstrated in Eq. (7) below:

$$Number = b_0 \cdot 2^0 + b_1 \cdot 2^1 + b_2 \cdot 2^2 + \cdots + b_{N-1} \cdot 2^{N-1} \tag{7}$$

here, b_0, LSB, and b_{N-1}, MSB, mathematically represent the lowest and highest weighted bits of a number in the binary system. For watermarking, watermark bits substitute the LSBs or MSBs of the pixels or coefficients. LSB has a lesser impact on the quality of the watermarked data compared to MSB, which affects it more.

Spherical coordinates transformation: Spherical coordinates are often used in 3D mesh and point cloud watermarking algorithms. Cartesian coordinates of a vertex are converted into spherical coordinates by using the following Eqs. (8)–(10) [41]:

$$\rho = \sqrt{(x-x_g)^2 + (y-y_g)^2 + (z-z_g)^2} \tag{8}$$

$$\theta = \tan^{-1} \frac{(y-y_g)}{(x-x_g)} \tag{9}$$

$$\phi = \cos^{-1} \frac{(z-z_g)}{\sqrt{(x-x_g)^2 + (y-y_g)^2 + (z-z_g)^2}} \tag{10}$$

here, (x, y, z) are the cartesian coordinates of a vertex, (x_g, y_g, z_g) is the center of gravity and, ρ, θ, ϕ are the vertex norm, azimuthal angle, and polar angle respectively. Watermarking for 3D meshes and point clouds usually utilizes vertex norms to embed the watermark. Alternatively, adjusting angles serves as a method to embed the watermark.

Normalization: This normalization adjusts the data such that the minimum value of the original dataset is transformed to 0 and the maximum to 1, while all intermediate values are scaled proportionally. The formula to normalize a value d from a given set is given in Eq. (11) as follows [42]:

$$d_{normalized} = \frac{d - d_{min}}{d_{max} - d_{min}} \tag{11}$$

where, d is the original value, d_{min} and d_{max} are minimum and maximum value in the set [42]. Normalization plays a crucial role in 3D mesh or point cloud watermarking, as it ensures that the watermark remains unaffected by the size of the model through radius normalization.

3.4. Some fundamental 3D watermarking algorithms

Here, we briefly outline key algorithms of 3D watermarking methods to guide new researchers.

Histogram mapping: Histogram mapping [41] is a primary method for 3D mesh and point cloud watermarking and serves as the basis for many other techniques. The embedding process, which involves embedding a watermark bit into a normalized bin, is outlined in Algorithm 1.

Algorithm 1 Histogram mapping [41]

1. Initialize real number parameter k_n as 1 to embed the watermark bit W_n into the nth bin, B_n.
2. Transform the normalized radii in the bin, B_n, by using Equation as follows:
$$r'_{n,\,k} = \left(r'_{n,\,k}\right)^{k_n}$$
3. If $W_n = 1$
   3.1. Calculate mean, μ_n,of transformed radii.
   3.2. If $\mu_n < \left(\frac{1}{2}\right) + \alpha$, decrease k_n $\left(k_n = k_n - \Delta k\right)$ and go to step 2. Otherwise, go to step 4.
   else
   3.3. Calculate the mean, μ_n, of transformed radii.
   3.4. If $\mu_n > \left(\frac{1}{2}\right) - \alpha$, increase k_n $\left(k_n = k_n + \Delta k\right)$ and go to step 2. Otherwise, go to step 4.
4. Replace normalized vertex norms with transformed norms.

Transform based algorithm: DWT and DCT are commonly used for 3D video and image watermarking. The fundamental DWT-based embedding process [43] is outlined in Algorithm 2.

LSB embedding: LSB is a classic and widely used algorithm in various media watermarking techniques. The basic LSB-based embedding process [43] is outlined in Algorithm 3.

4. Classification of attacks (research problem)

The robustness of watermarking methods against diverse attacks is a critical research area in the field. Evaluation of 3D watermarking

Table 2
Classification of attacks used in 3D watermarking.

Type	Attack classes	Examples
3D mesh	Content-preserving	Similarity transformations (rotation, translation, and uniform scaling) and file manipulations (reordering faces and vertices)
	Noise addition	Different types of noise, including Gaussian additive noise
	Filtering	Smoothing and sharpening
	Geometric	Cropping, vertex quantization, and compression
	Topological	Sampling, subdivision, remeshing, simplification, vertex addition, and vertex deletion
	Print-scan	Printing the digital 3D mesh using 3D printers and then scanning back into digital form
	Adversarial	Creating adversarial examples of watermarked data
	Temporal synchronization	Frame removal, insertion and swapping
3D image/video	Signal-processing	Compression, filtering, printing, scanning, and noise addition
	Geometric	Rotation, scaling, translation, stretching distortion (shearing), random bending, cropping, and row/column deletion
	Temporal synchronization	Frame removal, insertion and swapping
	Adversarial attacks	Creating adversarial examples of watermarked data
Point cloud	Content-preserving	Similarity transformations (rotation, translation, and uniform scaling) and file manipulations (reordering points)
	Noise addition	Different types of noise, including Gaussian additive noise
	Geometric	Cropping, simplification, point addition, and point deletion
	Temporal synchronization	Frame removal, insertion and swapping
NeRF	Rendering-based	Noise addition, cropping and filtering
	Model-based	Changing model weights, employing adversarial attacks, and modifying only the watermarking component of the trained deep model

Algorithm 2 Transform based [43]

1. Apply the 3rd level of the discrete wavelet transform (DWT) to the original view, O, and the watermark, W, using the following equations:

$$LL_1, LH_1, HL_1, HH_1 \leftarrow DWT(Image)$$

$$LL_2, LH_2, HL_2, HH_2 \leftarrow DWT(LL_1)$$
$$LL_3, LH_3, HL_3, HH_3 \leftarrow DWT(LL_2)$$

2. Embed the high-frequency coefficients, W_i, HH_{W3} of the watermark, W, into the high-frequency coefficients, C_i, HH_{O3} of the original view, O, with the strength factor, β, using the following equation:

$$C_i' = C_i + \beta * W_i$$

3. Obtain the watermarked views by applying the Inverse DWT (IDWT) to the watermarked and original coefficients as follows:

$$LL_2' \leftarrow IDWT(LL_3,\ LH_3, LH_3, HH_3')$$

$$LL_1' \leftarrow IDWT(LL_2', LH_2, LH_2, HH_2)$$
$$Watermarked Image \leftarrow IDWT(LL_1', LH_1, HL_1, HH_1)$$

Algorithm 3 LSB embedding [43]

1. Convert the coefficients, L, and watermark, W, to binary format.
2. Embed the watermark, W_i, into the least significant bit of the coefficients, C_i:
 for each coefficient
  If $LSB(C_i) = W_i$
   $LSB(C_i) \leftarrow 0$
  else
   $LSB(C_i) \leftarrow 1$
3. Reconstruct the watermarked coefficients L' using the modified LSBs.

methods depends on the specific characteristics of the 3D cover data. Table 2 summarizes the classification of attacks used in the evaluation of 3D watermarking.

3D mesh watermarking: The 3D mesh representation, comprising vertices, edges, and triangles, is fundamental in 3D modeling due to its direct connection to rendering and shading pipelines. Widely used in fields like computer-aided design, animation, and gaming, meshes facilitate efficient visualization and manipulation of complex shapes and surfaces. In industries such as entertainment and manufacturing, where 3D models are extensively shared, watermarking techniques are crucial. In 3D mesh watermarking, attacks can be classified into content-preserving, noise addition, filtering, simple geometric, topological, print-scan, adversarial, and temporal synchronization attacks. *Content-preserving attacks* involve actions such as similarity transformations (rotation, translation, and uniform scaling) and file manipulations (reordering faces and vertices) [31]. These attacks leave the content visually unchanged. *Noise addition attacks* encompass different types of noise, including Gaussian additive noise. *Filtering attacks* [34] involve smoothing and sharpening, while *Geometric attacks* [34] include cropping, vertex quantization, and compression. Filtering and geometric attacks can cause mesh elements to shift, reposition, or even be replaced. *Topological attacks* manipulate the connectivity details of the mesh and involve actions such as sampling, subdivision, remeshing, simplification, vertex addition, and vertex deletion applied to the 3D mesh [34]. A unique challenge for 3D mesh watermarking is the *print-scan attack*, where digital 3D meshes are printed using 3D printers and then scanned back into digital form [35]. The watermark extraction processes are then attempted on the scanned 3D mesh, making this one of the most challenging attacks for 3D mesh watermarking methods. *Adversarial attack* involves attacks designed to deceive deep learning-based 3D mesh watermarking methods by adversarial samples. These attacks aim to evaluate the robustness of the deep learning-based approaches. *Temporal synchronization attack* refer to the manipulation of frames of 3D dynamic mesh or frames of 3D mesh sequence in 4D data by removing, inserting, or swapping them [151].

3D image and video watermarking: 3D image and video data types include depth information alongside visual data, facilitating enhanced spatial understanding in applications like augmented reality,

Table 3
Classification of the 3D watermarking methods according to distortion.

	Lossy			Lossless		
Data type	Spatial	Transform	Deep learning	Zero-watermarking	Reversible	Storage features
3D mesh	[44], [45], [46], [47], [48], [49], [50], [51], [52], [53], [54], [55], [56], [57], [58], [59], [60], [61], [62], [63], [64], [65], [66], [67], [68], [69], [70], [71], [72], [73], [74], [75]	[76], [77], [78], [48], [79], [80], [81], [82], [83], [68], [84]	[85], [86], [87]	[88], [89], [90], [91]	[92], [93], [94], [95]	
3D video	[43], [96]	[97], [98], [99], [100], [101], [43], [102], [103], [104], [105], [96], [106], [107]		[108], [109], [110], [111], [112]		
3D image		[113], [114], [115], [116], [117], [118], [119], [120], [121], [122], [123], [124], [125], [126]	[127]			
Point cloud	[128], [129], [130], [131], [132], [133], [134], [135], [136]	[137], [138]		[135]		[139]
NeRF			[140], [141], [142], [143], [144], [145], [146], [147], [148], [149], [150]			

virtual reality, and computer vision. They find applications in gaming, medical imaging, robotics, and surveillance. As their usage expands across industries such as entertainment, manufacturing, and defense, robust watermarking techniques become essential for protecting intellectual property and ensuring data integrity. To gauge the robustness of watermarking, a group of attacks can be used. It includes typical signal-processing attacks, geometric attacks, temporal synchronization attacks, and adversarial attacks. *Signal-processing attacks* involve compression, filtering, printing, scanning, and noise addition [32]. *Temporal synchronization attacks* encompass the frame removal, insertion and swapping [12]. *Geometric attacks* manipulate the spatial attributes of an image, incorporating both local and global alterations. Global geometric attacks encompass fundamental transformations such as rotation, scaling, translation, stretching distortion (shearing), as well as other affine and projection transformations. In contrast, local geometric attacks involve random bending, cropping, and row/column deletion [32]. It is crucial to recognize that, unlike 3D meshes, these geometric operations – like rotation, scaling, and translation – are not readily reversible on images due to their regular structure. Consequently, they do not preserve the content of the original image. For example, translating an image beyond its canvas leads to the loss of pixel information. *Adversarial attacks* are targeted specifically at learning-based watermarking algorithms [32]. They involve generating adversarial examples of watermarked data with the intention of deceiving the trained network. Such attacks are employed to manipulate learning-based methods into generating incorrect results and exploit the vulnerabilities inherent in these methods [152].

Point Cloud Watermarking: A point cloud is a collection of unordered points that represent objects or scenes in three-dimensional space. This 3D representation has garnered substantial research interest due to recent advancements in sensor devices, such as LiDAR, and improvements in capturing and processing techniques. Particularly noteworthy is the development of deep learning backbones like PointNet [153], PointNet++ [154], DGCNN [155], among others, which have allowed point clouds to become a versatile 3D representation in both research and industries. The ability to handle large-scale data and complex spatial relationships makes point clouds invaluable for various applications ranging from autonomous driving to virtual reality. As the utilization of point clouds continues to expand, the need for robust watermarking techniques becomes increasingly apparent. The attacks employed to assess point cloud watermarking techniques, including simplification, noise addition, content-preserving actions, cropping, as well as point addition and deletion, closely resemble those utilized in the classification and evaluation of 3D mesh watermarking [128,131,138], namely *Content-preserving, Noise addition, and Geometric*. Also, *Temporal synchronization* attacks refer to deliberate acts of tampering with the frames in the dynamic point cloud, such as removal, insertion, and swapping. It is important to note that face and edge-based attacks, commonly applied in the context of 3D meshes, are not applicable to point cloud methods given their distinct nature (sets of unordered

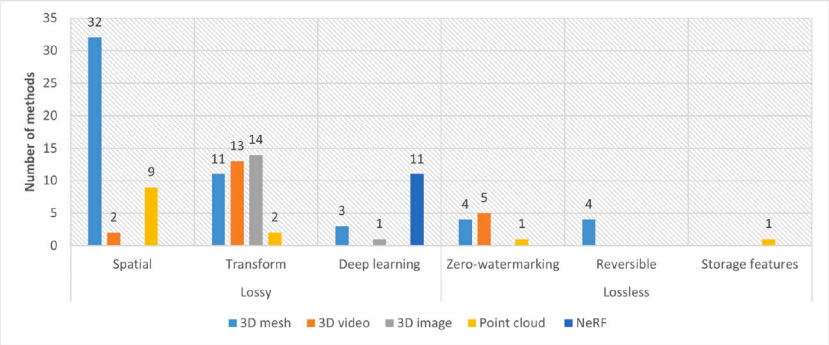

Fig. 3. Distribution of the techniques according to distortion and data type.

points). Additionally, topological attacks are not applicable to point clouds as they do not involve any inherent connectivities between points, unlike the vertices found in 3D meshes.

NeRF watermarking: NeRF (Neural Radiance Fields) is a revolutionary method in 3D modeling and rendering [36]. Its flexibility and high fidelity for novel view synthesis, coupled with its capacity for data disentanglement through deep learning, have ignited significant interest in representing both 3D static and dynamic scenes. This, in turn, has fueled recent interest in watermarking within the NeRF framework. Attacks in the NeRF watermarking can be categorized into two main types: rendering-based attacks and model-based attacks. *Rendering-based attacks* encompass various techniques used in 2D image watermarking algorithms, such as noise addition, cropping, and filtering [140]. In contrast, *model-based attacks* involve manipulating the model itself, including changing model weights, employing adversarial attacks, and modifying only the watermarking component of the trained deep model [140].

5. Classification of techniques by distortion

Here, we classify each type of 3D watermarking method according to distortion and data type. Table 3 shows the classification of the 3D watermarking methods. Lossy watermarking methods introduce some degree of distortion to embed watermarks, while lossless methods preserve the original data without any alteration [89]. Within the lossy category, techniques include spatial, transform, and deep learning methods, whereas lossless techniques encompass zero-watermarking and reversible, storage features.

Lossy watermarking algorithms are conventional methods that embed watermarks into the cover data. During the embedding process, certain parts of the original cover data are altered, hence the term "lossy" algorithms. These techniques can be further classified into spatial, transform, and deep learning methods based on their embedding domains. In the *spatial* domain, methods embed the watermark directly into the image plane itself [96] or modify the geometry [47] or connectivity of the 3D shapes [68]. In the *transform* domain, methods embed the watermark in the harmonic coefficients [80] or coefficients of frequency or wavelet [78]. Conversely, *deep learning-based* methods embed the watermark into spatial or transform domains or both using neural networks [87].

Lossless watermarking algorithms provide copyright protection for data without compromising its accuracy or quality [139]. These techniques can be further classified into zero-watermarking, reversible watermarking, and storage features-based watermarking. *Zero watermarking* methods do not embed the watermark into the cover model. Instead, unique features are extracted from the data without modifying the cover data. The extracted watermarks are registered and stored in the intellectual property rights (IPR) database, ensuring that the protected data remains undistorted throughout the watermarking process. *Reversible watermarking* methods enable the complete extraction of the watermark and restoration of the cover data [156]. This ensures that not only can the watermark be easily retrieved, but the watermarked data can also be fully restored to its original state with no loss of quality, thus maintaining the originality of the data. *Storage features-based* watermarking methods, initially proposed for vector data [157], embed the watermark into the data without altering the coordinate values. They utilize specific rules to modify the storage order of the data, ensuring the lossless embedding of the watermark [139].

Observations: Table 3 reveals trends in 3D watermarking research. There are more lossy than lossless techniques, highlighting a focus on embedding-based approaches, as also shown in Fig. 3. Spatial domain methods dominate in 3D mesh and point cloud watermarking, while transform domain methods are more common in 3D video and image watermarking due to their regularity and ease of implementation. Deep learning-based methods remain limited, though NeRF watermarking exclusively uses them. In lossless watermarking, zero watermarking has garnered more attention than reversible or storage feature-based methods, with only one storage feature-based method available for 3D watermarking, applicable only to vector-type data.

6. Classification based on the technical properties

While Section 5 discusses techniques based on distortion, we offer a more detailed breakdown according to the technical properties utilized by these techniques. We follow the order as listed in Table 3: spatial, transform, deep learning, zero watermarking, reversible, and storage features. The detailed classification based on technical properties is demonstrated in Fig. 4.

6.1. Spatial

Spatial domain watermarking methods utilize the spatial properties of the cover data, including geometry, connectivity, and pixel value, to embed the watermark. Table 4 survey these common technical properties, and we discuss them below.

Histogram mapping: The histogram mapping function, introduced by Cho et al. [41], modifies the mean or variance values of bins within a histogram of vertex properties to embed a watermark. Very often, 3D data are transformed into spherical coordinate. To embed a watermark bit of 1 (0), the vertex norms (radii) in the bin are modified so that its mean value is greater (smaller) than the reference value. Several methods [47,49,51,54–56,62,63,67,69,70,75] use this histogram mapping function, its improved variations, or slight modifications to embed watermarks into 3D meshes. Although some of these methods address different issues, such as being resilient to cropping [49,62] or print-scan processes [51], they fundamentally embed watermarks by altering the mean or variance values of bins. Similarly, some point cloud watermarking methods [128,131] apply variations of the histogram mapping function introduced by Cho et al. [41]. Jin and Kim [44] proposed

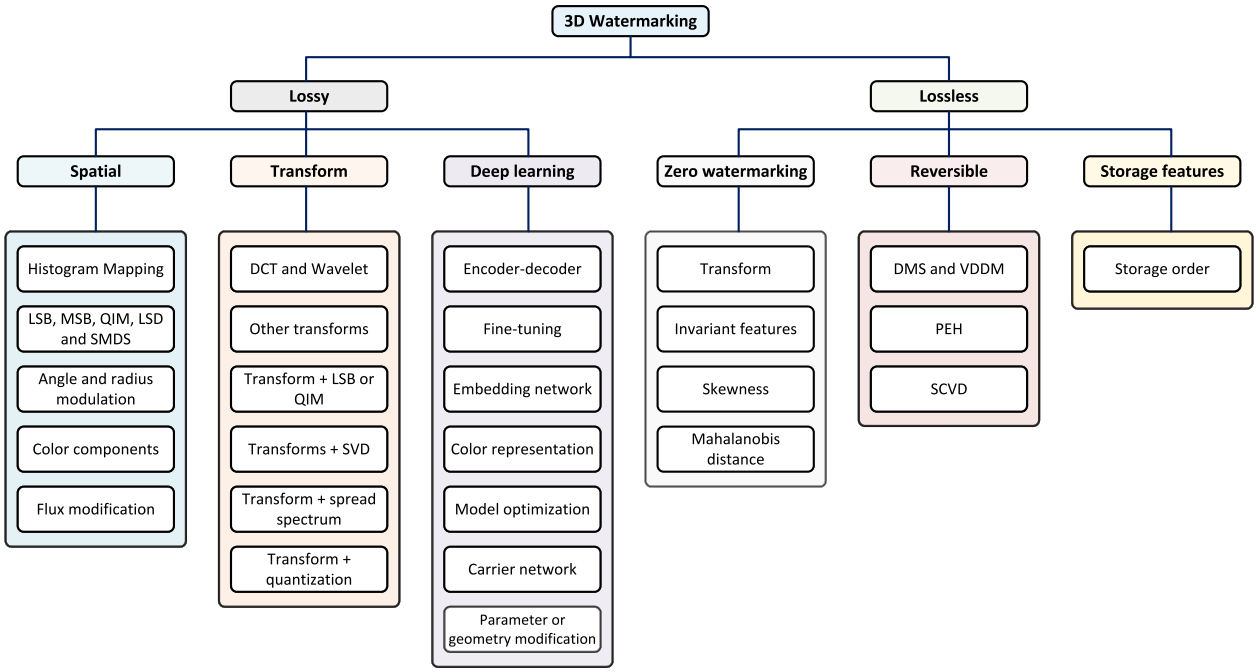

Fig. 4. Classification based on technical properties.

Table 4
Classification of the spatial based 3D watermarking methods according to technical properties.

Spatial	Methods
Histogram mapping	[47], [49], [51], [54], [55], [56], [62], [63], [69], [70], [67], [44], [131], [128], [75]
LSB, MSB, QIM, LSD and SMDS	[46], [45], [53], [60], [133], [43], [96], [58], [74]
Angle and radius modulation	[129], [132], [130]
Color components	[66], [135]
Angle, radius, vertex modification	[61], [71], [52],[65], [64], [50], [57], [72], [136]
Flux modification	[73]

a CityGML model watermarking method based on coordinate quantization transformation. In this method, selected vertices are quantized within a given space, and the watermark is inserted by modifying the mean values in a manner similar to the histogram mapping function.

LSB, MSB, QIM, LSD and SMDS: The Least Significant Bit (LSB) and Most Significant Bit (MSB) methods are widely adopted spatial domain techniques, altering the least and most significant bits of the cover data components, respectively. Quantization Index Modulation (QIM) is also a popular spatial embedding strategy along with LSB. It is a two-stage process. Initially, QIM determines the quantization levels, which are the distinct values a signal may assume post-quantization, in accordance with the bits of information intended for embedding. Subsequently, by modulating these indices, the signal is able to convey watermark data subtly, without markedly altering its fundamental attributes. In 3D mesh watermarking, [46] embeds watermarks into the MSB region of the mantissa part of vertex coordinates, while [45] utilizes LSBs for embedding chaos-based watermarks. Similarly, [53] employs the least significant decimal points (LSD) of vertices, and [60] modifies vertex coordinates using simple message-digit substitution (SMDS). Conversely, [74] utilizes QIM for the embedding of watermarks. For point cloud watermarking, [133] proposes a framework integrating traditional strategies like LSB and quantization index modulation (QIM). Conversely, spatial-based methods for 3D video watermarking predominantly employ LSB techniques; in [43], LSB is applied to the lightness coefficient of right and left views, while [96] embeds watermarks into red image frames of 3D anaglyph videos using LSB. Additionally, [58] utilizes dithering and angle quantization index modulation for watermark embedding.

Angle and radius modulation: These techniques modulate azimuth angles or radius to embed the watermark. In modulation techniques, each ball ring or distinct region is divided into two sub-regions, and the number of angles or radius in the sub-regions are increased or decreased according to some equation to embed the watermark (‘0’,‘1’) into the ball ring or region. Among point cloud watermarking methods, only three utilize modulation. [129,132] embed the watermark into bins by modulating azimuth angles of feature vertices using a modulating parameter, while [130] embeds the watermark into the ball ring by modulating the radial radius.

Color components: Color components-based watermarking techniques modify the color information of vertices or points. [66] describes a method that converts a mesh into a geometry image, where watermark bits are embedded into the color components of the pixels. The embedding process depends on whether the region of the geometry image, derived from the cover mesh, is a protrusion or a concave area. [135] inserts the watermark into the color information of feature points obtained using intrinsic shape signatures.

Angles, radius, vertex modification: These techniques modify angles, radius, or vertices to embed the watermark. [61] embeds the watermark by modifying the radius component of the vertices, while [71] embeds a spread-spectrum signal generated with the watermark and

Table 5
Classification of the transform based 3D watermarking methods according to technical properties.

Transform	Methods
DCT and Wavelet	[77], [79], [48], [68], [82], [83], [70], [113], [120], [117], [100], [43], [96], [106], [107], [104], [103],[105], [98]
Other transforms	[76], [80], [81], [119], [115]
Transform + LSB or QIM	[76], [80], [81], [78], [106]
Transforms + SVD	[99], [101], [103], [105], [116], [126]
Transform + spread spectrum	[97], [102], [118],[121], [124], [125]
Transform + quantization	[114], [123]

azimuth angle into the radius of vertices after spherical transformation. [52] inserts the generated watermark signal into selected robust locations by modifying positions in the normal direction. [65] embeds the watermark values by modifying both the azimuthal and polar angles. [64] embeds a watermark directly into the mesh by delicately scaling the vertices. Additionally, it employs statistical analysis of the 1-ring neighborhood to enhance the watermarking process. [50] converts the vertices from 3D coordinates to 2D coordinates and embeds the watermark by modifying the third vertex point in the 2D coordinates. [57] embeds the bits of a secret logo using a vertex-shifting method, which moves the coordinates of the vertex according to watermark bits and shift values. [72] embeds the watermark into the embedded primitive points using the strength factor. [136] embeds the watermark into the coordinates in the subregion by applying a positive or negative displacement value according to the height of the subregion and the average of the points.

Flux modification: These techniques embed the watermark into the flux of a vector field across the model's surface. [73] embeds the watermark into the flux to get a new flux using the scaling parameter. Then, this method perturbs the vertices on the mesh so that the vertices are adjusted to achieve the altered flux values to embed the watermark into the mesh model.

In general, these selected methods offer several benefits for watermarking:

- Histogram mapping method for 3D mesh and point cloud data allows watermarks to withstand common attacks such as vertex reordering and similarity transforms [41] while modulation techniques can withstand attacks like addictive noise and rotation [129,132]. Modulation techniques can also be applied to vertices in 3D meshes to protect copyright [129,130,132].
- Methods that modify LSB or use color information often ensure the watermark is not visible to users, preserving the visual quality of the 3D model [45,135].
- Embedding strategies that involve complex operations or secure layers, such as using an encrypted watermark or a chaos sequence-based watermark, add a level of protection against unauthorized claims or removal [45,53].
- Different properties, such as angle and radius, and methods, like histogram mapping, used for 3D mesh allow for application-specific adaptations, such as those required for point clouds [128, 131].

6.2. Transform

Transform-based methods embed watermarks by modifying the coefficients of various transforms applied to the 3D data. This process involves converting the data into transform coefficients (e.g., frequencies) and embedding the watermark within these coefficients. Typically, this is achieved through mathematical operations such as addition and subtraction, sometimes incorporating a strength factor. By embedding the watermark in the transform coefficients, the visual quality of the 3D model is preserved, making the watermark imperceptible to the human eye. The watermark can be recovered by applying the inverse transform and detecting the specific changes made to the coefficients. Table 5 surveys these common methods.

DCT and Wavelet: DCT and Wavelet transform are widely used because they provide a mean to embed watermarks into the frequency component of the cover data, which are less perceptible to the human eye when slightly modified. Modifying mid-frequency DCT coefficients tends to balance robustness and imperceptibility [158]. DWT provides multi-resolution analysis, allowing watermarks to be embedded in various frequency bands. Most of the DCT and wavelet based methods insert the watermark into the coefficient using an equation, basically adding and subtraction, etc, with or without the strength factor. In 3D mesh watermarking, [48,68,77,79] use the DCT coefficients, while [70,82,83] use the wavelet coefficients as embedding domain. In 3D image watermarking, [113,120] insert the watermark into the coefficient of the DCT transform, while [117] uses the DWT coefficient for embedding. In 3D video watermarking, [43,96,100,106,107] use the DWT coefficients to embed the watermark. [43,96] also use the DCT coefficients to embed another watermark, which is different from those used in DWT embedding. [104] uses the Krawtchouk moments and DCT coefficients to insert the watermark. [103,105] have DCT and discrete stationary wavelet transform (DSWT) based embedding. [98] embeds the watermark into level 3 complex coefficients of the dualtree complex wavelet transform (DT CWT) decomposition.

Other transforms: Other than the DCT and wavelet, some of the 3D watermarking methods use the spherical harmonics decomposition, unlifted butterfly wavelet transform, and digital shearlet transform. [76, 80] utilize the spherical harmonics decomposition, whereas [81] applies the unlifted butterfly wavelet transform as its transformation method. [119] embeds the watermark into the low-frequency component of Gaussian filtering by consolidating histogram shape-based embedding. [115] embeds the watermark into the digital shearlet transform-maximum noise fraction band by using the embedding equation with modulation factor.

Transform + LSB or QIM: LSB and QIM, popular spatial domain embedding methods, are used to embed the watermark into the transform coefficient. [76,80,81] use the LSB modification to embed the watermark after the transform, while [78] uses the QIM to embed the watermark into the wavelet coefficients. [106] also embeds another watermark by using the LSB embedding in DWT coefficients.

Transforms + SVD: Singular Value Decomposition (SVD) is a fundamental matrix factorization technique used in digital watermarking and several other areas, such as statistics, signal processing, and machine learning. A small number of singular values can effectively express a large fraction of the signal energy, making the process of extracting a watermark efficient and ensuring that the extracted watermark maintains high quality even after withstanding various attacks [159]. Additionally, watermarking in the hybrid domain (combining Transform and SVD) is extremely difficult to remove or alter without causing damage to the original data. Embedding the watermark using the SVD domain results in high imperceptibility in the cover data, even

Table 6
Classification of the deep learning based 3D watermarking methods according to technical properties.

Deep Learning	Methods
Encoder–decoder	[85], [86], [127]
Fine-tuning	[143]
Embedding network	[87], [142], [150]
Color representation	[140]
Model optimization	[141], [146], [147], [149]
Carrier network	[144]
Parameter or geometry modification	[145], [148]

after modification [159]. Moreover, using SVD after DCT or DWT can increase security, and this multi-stage process creates a more complex embedding scheme, making it harder for attackers to detect and remove the watermark. SVD is commonly used for image and video watermarking with several transforms. In 3D image and video watermarking, some of the methods use one or two transforms before singular value decomposition (SVD) and then embed the watermark into to coefficient of SVD. [99] uses the DWT before SVD, [101] uses the Motion compensated DCT before SVD, while [103,105] use the DWT and Homomorphic before SVD to embed the watermark. [116, 126] embed the watermark into the integer wavelet transform using the lifting scheme and the singular value decomposition (SVD) and DWT-SVD coefficients, respectively.

Transform + spread spectrum: Spread spectrum watermarking involves spreading the watermark signal over a broad range of frequencies or spatial locations. ISS is an improved version of secret spectrum embedding, which reduces interference while embedding, improving the quality of the watermarking process [118,160]. Spread spectrum and improved spread spectrum (ISS) are used to embed the watermark into the transform coefficients in 3D video and image watermarking. In 3D video watermarking, [97] embeds the watermark into the high band frequency of DCT coefficients by using the spread spectrum embedding, while [102] embeds the watermark into the AC coefficients of DCT by using improved spread spectrum (ISS). In 3D image watermarking, [118,121] use the ISS in DCT and [124] uses the ISS ın DWT while [125] uses the spread spectrum embedding in DCT coefficients like [118,121,124].

Transform + quantization: These methods embed the watermark into coefficients by modifying the quantization levels. [114,123] use the quantization-based embedding in non-subsampled contourlet transform and dual-tree complex wavelet transform, respectively.

In general, these techniques offer several benefits for watermarking:

- Transforms like DCT and DWT provide robustness against common operations such as compression, noise, and various types of distortions, ensuring the watermark remains intact, especially for 3D video and image [43,113].
- Embedding in transform domains typically results in changes that are not easily perceptible to the human eye, maintaining the visual quality of the 3D model.
- Different transforms can be applied to various types of data (e.g., meshes, images, videos, point clouds), allowing for flexible watermarking solutions tailored to specific applications.

6.3. Deep learning

Deep learning-based 3D watermarking efficiently embeds watermarks into the cover data using architectures such as encoder–decoder. There are only three for 3D mesh, one for 3D image, and 4 for NeRF watermarking methods based on deep learning. Table 6 surveys these deep-learning strategies for watermarking.

Encoder–decoder: An encoder–decoder is a deep learning architecture designed to embed a watermark into a host signal and later extract the watermark from the watermarked signal. There are two encoder-based watermarking methods for 3D mesh watermarking and one method for 3D image watermarking. [85] embeds the watermark into vertex and texture components, while [86] embeds binary messages in vertex distributions. Both methods optimize the networks with a respective loss function to effectively embed and extract the watermark information. In 3D image watermarking, [127] embeds the watermark into the center view of the 3D image using an encoder that incorporates a bilateral attention module.

Fine-tuning: Fine-tuning plays a pivotal role in deep learning, serving to adjust a pre-trained model to a specialized task. Presently, there is one method exists that employs fine-tuning for watermarking within the context of Neural Radiance Fields (NeRF) [143]. It incorporates a watermark directly into the NeRF model's weights through a process of fine-tuning.

Embedding network: Apart from the encoder–decoder architecture, three techniques employ bespoke embedding networks for 3D watermarking. [87] introduces a watermark into the vertex component through a specialized watermark embedding sub-network. In contrast, [142] implements watermarking into the training images of the NeRF model using an embedding network. Similarly, [150] embeds the watermark into the training images.

Color representation: Instead of embedding the watermark in the vertex or texture components, [140] develops a novel approach to embed messages into the NeRF network by creating a watermarked color representation. During training, it deploys a distortion-resistant rendering module to map the geometry and watermarked color representations to image patches. Subsequently, a CNN-based message extractor is used to decode the secret message.

Model optimization: An alternative approach for NeRF watermarking involves optimizing the model to embed the watermark. To do so, [141] strategically injects the watermark into the NeRF model's less significant weights through weight optimization. [147] embeds the watermark into the NeRF model using a two-stage optimization process, incorporating a digital signature into the model's weights through the sign loss objective. [149] introduced a plug-and-play method for watermarking NeRF during the creation phase, using message distillation and Progressive Global Rendering. [146] optimizes the NeRF model to ensure accurate decoding of the watermark message from rendered images via a decoder.

Parameter or geometry modification: A different approach for NeRF watermarking, [145] embeds the watermark by adding signature representation into the original NeRF model parameters element-wise. This method splits the parameters into two parts, using one section for embedding. In contrast, [148] attaches a binary watermark into high-geometry value components, ensuring robustness against recolorization due to the use of geometry values.

Carrier network: [144] introduces a watermarking technique utilizing a carrier network. Here, a NeRF model serves as the watermark, embedded within another carrier NeRF model. The process involves initially expanding the watermark network by inserting new nodes and layers using vertical, horizontal, or mixed expansion strategies to form the carrier network. These strategies aim to preserve the structure of the watermark network. Subsequently, the carrier model undergoes training to represent a new cover NeRF model while keeping the watermark network frozen.

In general, these deep-learning-based techniques offer several benefits:

- Encoder–decoder architectures and embedding network modules allow for efficient embedding and extraction of watermarks while preserving the visual quality of the 3D data [87,127].
- Deep learning based methods can be improved or fine-tuned according to the actual requirements via changing the attacks in the attack or distortion layers [87,140].

Table 7
Classification of the zero watermark based 3D watermarking methods according to technical properties.

Zero Watermark	Methods
Transform	[110], [109], [111], [112], [88]
Invariant features	[108]
Skewness	[90], [91], [89]
Mahalanobis distance	[135]

- Embedding watermarks directly into model weights in NeRF watermarking methods enables robust copyright protection while maintaining compatibility with existing NeRF models [140,143].

6.4. Zero watermarking

Zero-watermarking is a technique that diverges from traditional watermarking methods. Instead of directly embedding the watermark into the host signal, these methods extract distinctive features from the host signal and merge them with the watermark information to form a zero-watermark. This zero-watermark is subsequently stored in a secure location, such as an IPR database. Table 7 presents the classification of zero watermark methods based on technical properties.

Transform: Transform-based zero watermarking methods utilize features derived from transforms such as DCT and contourlet transform. [110] generates the zero-watermark through attention-based fusion of Discrete Cosine Transform (DCT) features and features based on the Dual-tree complex wavelet transform. [109] employs the low-frequency coefficients of DCT-applied Temporally Informative Representative Images (TIRIs) of frames and deep maps to produce content-based features for generating the zero-watermark. [111,112] generate the zero-watermark using the contourlet transform and features obtained from singular value decomposition. An enhanced version of [111,112], utilizes a logistic chaotic system to encrypt the designed features and improve the geometric rectification mechanism. [88] introduces the Beamlet transform to construct the zero-watermarking image.

Invariant features: Invariant features, crucial for robustness against signal and geometrical attacks, as well as depth-image-based rendering, are obtained from 2D frames and depth maps. These features, computed as centroids of normalized variations between video frames and informative images, are utilized by [108] for copyright protection in 3D video, generating master and ownership shares.

Skewness: Skewness is a measurement that can indicate whether a group distribution is symmetrical [89]. There are three zero-watermarking methods in 3D mesh watermarking based on skewness. [90] generates the zero-watermark by using the skewness values of the angles in bins. [91] produces the zero watermark from multi-features, which are constructed from skewness obtained from the SDF value partitions, skewness from vertex norm partitions, and the ratio of the number of vertices. [89] combines the dominant and recessive features obtained from gene groups as a unique gene feature-based zero watermark.

Mahalanobis distance: Mahalanobis distance is a statistical-based distance measure that takes into account the correlation of datasets. [135] uses the Mahalanobis distance to construct the feature matrix of point cloud data, and then a zero watermark is generated by executing the XOR operation between the feature matrix and binary watermark image.

Zero watermarking methods in general offer several benefits:

- Zero watermarking ensures the originality of the data remains undistorted throughout the watermarking process because the watermark is stored in the IPR database.
- Features extracted from 3D data using transform, are robust against signal processing and DIBR based attacks and alterations, ensuring the ownership of the content [110–112].
- Techniques like encryption and chaotic systems enhance the security of zero watermarking, making it challenging for unauthorized parties [110,112].

Table 8
Classification of the reversible 3D watermarking methods according to technical properties.

Reversible	Methods
DMS and VDDM	[94], [93]
PEH	[95]
SCVD	[92]

6.5. Reversible

Reversible watermarking techniques facilitate the extraction of unaltered cover data after watermark extraction, ensuring lossless recovery. These methods typically embed the watermark in a reversible manner, allowing for accurate restoration of the original cover data without any perceptible distortion or loss of information. Table 8 presents the classification of reversible methods based on technical properties.

DMS and VDDM: Double modulation strategy (DMS) and variable direction double modulation (VDDM) are watermark embedding strategies developed based on improved quantization index. [94] utilizes DMS for watermark embedding, involving vertex modulation based on motion direction. Additionally, [93] employs VDDM, an extension of IQIM, for the same purpose. It generates the watermark based on one-ring neighborhood unlike the single-vertex-based watermark generation. It then embeds the watermark in both the encrypted domain and plaintext domain of 3D mesh, allowing authentication in both domains.

Prediction Error Histogram (PEH): The core concept of the PEH is to leverage the spatial redundancy inherent in the attributes of a 3D model or an image to embed binary bits in a reversible manner. In [95], the watermark is inserted into the embeddable unit using the PEH modification technique, where the PEH is generated using the vertex normal value ordering strategy.

Spherical Crown Volume Division (SCVD): The SCVD technique, in which vertices are mapped into circles with varying radii, leverages the properties of the sphere to create a more aggregated distribution of embedded vertices with the original ones. In [92], an embedding strategy based on SCVD is proposed, where watermark insertion is accomplished by modifying the calculated virtual arc on the sphere.

Employing these techniques offers several benefits:

- Reversible watermarking ensures lossless recovery of the original data after watermark extraction, making it suitable for applications where data integrity is critical.
- Techniques using prediction error histogram modification and spherical crown volume division minimize perceptual distortion, ensuring that the embedded watermark does not significantly affect the visual quality of the data [92,95].
- The use of techniques such as double modulation and variable direction double modulation effectively minimizes embedding distortion. Approaches utilizing DMS and VDDM have shown good performance in achieving semi-fragility, imperceptibility, and accurate tampering location detection [93,94].

6.6. Storage features

Storage feature-based watermarking, originally designed for vector data, embeds the watermark into the data without modifying its values. This is achieved by applying specific rules to rearrange the data storage, ensuring that the watermark is embedded without loss. While this

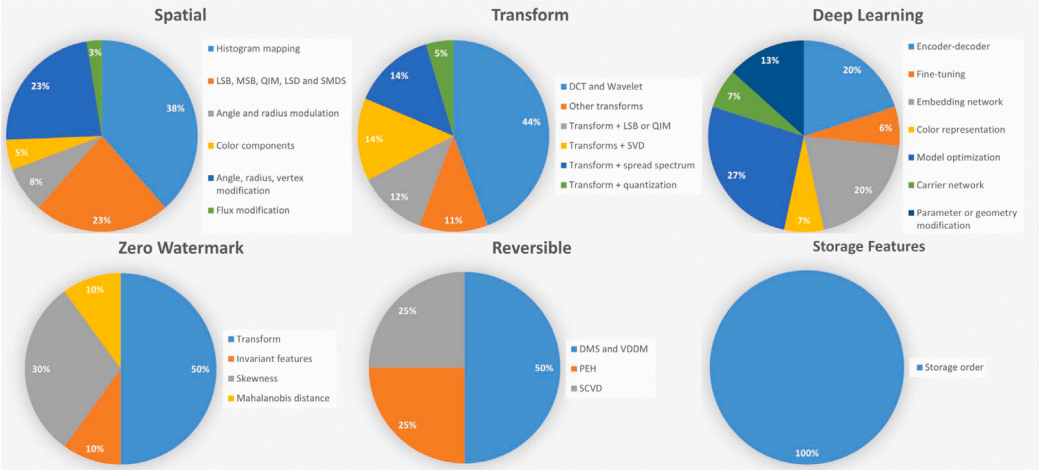

Fig. 5. Distribution of the techniques in classification according to technical properties.

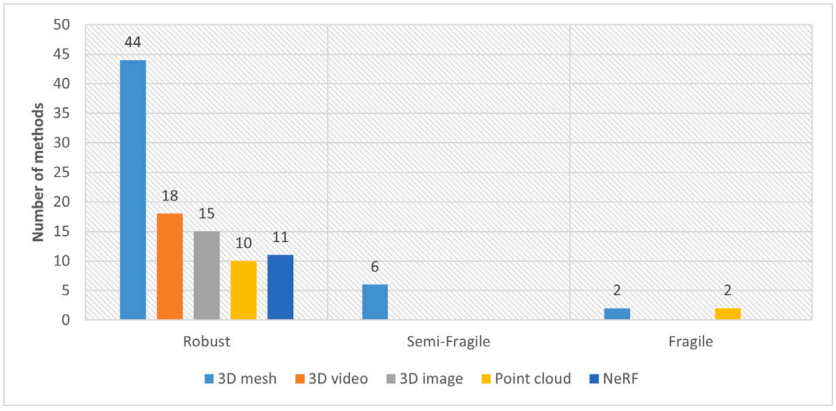

Fig. 6. Distribution of the techniques according to robustness.

technique is primarily utilized for vector data, there exists one 3D watermarking method specifically proposed for point cloud data.

Storage order: The relative storage order of geospatial point cloud data is one of the invariant features. [139] embeds the watermark by modifying the relative storage order according to the watermark and index value without altering the coordinate values. This methods achieve traceability and can protect the copyright under the lossless precision.

In general, storage feature-based watermarking offers several benefits:

- The storage order of the point cloud data can remain unchanged after noise, transformation, and geometric attacks [139].
- These techniques ensure that the originality of the cover data remains distortionless even after the watermarking process [139].

6.7. Distribution of the techniques in each category

Fig. 5 shows the distribution of techniques by technical properties. Histogram mapping leads in the spatial category, while DCT and Wavelet based methods dominate in transform-based watermarking. In deep learning, model optimization-based embedding is more common. Transform-based methods represent half of zero watermarking studies, and storage order-based techniques are the sole method in the storage features category. DMS and VDDM make up half of reversible watermarking studies.

7. Classification of techniques by robustness

We classify each type of 3D watermarking method according to robustness and data type in this section. Table 9 demonstrates the classification of the 3D watermarking method. Also, the distribution of the techniques according to robustness and data type is shown in Fig. 6. As mentioned in Section 3.1, robust watermarking algorithms focus on high capacity, more robustness, and fewer distortions. Semi-fragile and fragile methods focus on high imperceptibility and tampering detection accuracy. Table 9 and Fig. 6 shows that researchers are more focused on robust watermarking than semi-fragile and fragile watermarking. It also shows that research is solely made on robust watermarking for 3D image/video and NeRF. In Table 10, we further summarize the pros and cons for each data type of watermarking method. Below, we mention our observations for each type of 3D watermarking.

3D Meshes: Table 9 shows the number of fragile and semi-fragile methods in 3D mesh watermarking is lower than robust methods. Table 10 shows that many methods are vulnerable to cropping attacks [50,57,62,67,70,78,88,90,95], have low capacity [52,55,86], and have non-blindness [64,83]. Most of them are also not evaluated for print scan attacks whilst some new methods [51,52,71] are focusing on this issue. We also observe that some have good imperceptibility [55,56,73,78], no distortions [88–91] and high capacity [46,53,59,60,76,77,79,80,83] while other focus on the trade-off between robustness and imperceptibility [48,61,73,78]. Methods, in general, are robust against various attacks [49,51,52,55,56,62,64,66,69,71,89,90].

Table 9
Classification of the 3D watermarking methods according to robustness.

Data type	Robust	Semi-Fragile	Fragile
3D mesh	[85], [76], [77], [44], [46], [78], [47], [48], [49], [79], [80], [86], [71], [88], [89], [50], [51], [52], [53], [87], [54], [90], [55], [81], [56], [57], [91], [59], [61], [62], [82], [63], [64], [65], [66], [83], [67], [68], [69], [70], [84], [72], [74], [75]	[92], [93], [94], [95], [58], [73]	[45], [60]
3D video	[108], [110], [109], [97], [98], [99], [100], [101], [43], [102], [103], [104], [105], [111], [112], [96], [106], [107]		
3D image	[127], [113], [114], [115], [116], [117], [118], [119], [120], [121], [122], [123], [124], [125], [126]		
Point cloud	[137], [128], [129], [130], [138], [139], [131], [132], [134], [135]		[133], [136]
NeRF	[140], [141], [142], [143], [144], [145], [146], [147], [148], [149], [150]		

Table 10
Drawbacks and advantages of the 3D watermarking methods.

Data type	Drawbacks	Methods	Advantages	Methods
3D mesh	Limitation against cropping or strong cropping attacks	[78], [88], [50], [90], [95], [57], [62], [67], [70]	Robustness to print-scan attacks	[71], [51], [52]
	Capacity	[86], [52], [55]	Robustness to cropping attacks	[49], [89], [55], [56], [61], [62], [64], [66], [69], [72], [74]
	Non-blindness	[64], [83]	High capacity	[76], [77], [46], [79], [80], [53], [59], [60], [83]
	Lack of evaluated for print scan attacks	All except [71], [51], [52]	Trade off between the robustness and imperceptibility	[78], [48], [61], [73]
	Complexity	[85], [86], [87], [73]	Good imperceptibility	[78], [55], [56] [73]
			No distortion	[88], [89], [90], [91]
3D video	Vulnerability against some attacks	[108], [109], [97], [98], [100], [96], [107]	Good imperceptibility	[99], [100], [105]
	Non-blindness	[103], [104], [105]	No distortion	[108], [109], [110],[111], [112]
	Need to register and store the watermark	[108], [110], [109], [111], [112]	Robustness to geometric attacks	[108], [110], [98], [100], [101], [104], [111], [96], [107]
	Lack of evaluated for combined attacks	All except [98], [107]	Robustness to signal processing attacks	[108], [97], [104], [105], [112], [107]
			Evaluated for combined attacks	[107], [98]
3D image	Capacity	[127], [117], [119], [125]	Good imperceptibility	[125], [123], [127], [113], [114], [122], [120]
	Vulnerability against some attacks	[114], [115], [116], [118], [121], [123], [126]	Optimum strength factor	[115]
	Needing high computing power	[115], [122]	Robustness to geometric attacks	[113], [116], [119], [122], [123], [124], [126], [125]
	Intuitively selecting the strength factor	[120], [116], [126]	Robustness to signal processing attacks	[113], [116], [120], [122], [123], [124], [126], [125]
	Complexity	[127]	Evaluated for combined attacks	[127], [116], [119], [125], [124], [121]
	Lack of evaluated for combined attacks	All except [127], [116], [119], [125], [124], [121]		
Point cloud	Limitation against cropping or strong cropping attacks	[129], [130], [131], [132]	Good imperceptibility	[128], [129], [134]
	Non-blindness	[137], [128]	Trade off between imperceptibility and robustness	[131], [129]
	Calculation burden	[133]	No distortion	[139]
	Limited against noise attacks	[138], [134]	Robustness to cropping attacks	[137], [138], [134]
	Lack of evaluated for print scan attacks	All		

3D Video: Table 9 shows that researchers focus mainly on robust 3D video watermarking techniques so far. Among them, [108–112] are zero watermarking techniques (Table 3). These methods need to register and store the watermark in the IPR database (Table 10). Therefore, the security of the database is one of the essential tasks for these methods. Further, Table 10 shows that the drawbacks of most methods are vulnerability against some attacks [96–98,100,107–109], non-blindness problems [103–105] and lack of evaluation against combined attacks (all except [98,107]). Some of the methods have good imperceptibility [99,100,105], no distortions [108–112] while some have robustness against geometric [96,98,100,101,104,107,108,110,111] and signal processing [97,104,105,107,108,112] attacks.

3D image: Table 9 shows that researchers focus on only robust 3D image watermarking techniques. Table 10 shows that the methods have limitations such as capacity [117,119,125,127], vulnerability against some attacks [114–116,118,121,123,126], needing high computing power [115,122], complexity [127] and intuitively selecting the strength factor [116,120,126]. Also, some of them were not evaluated against combined attacks (all except [116,119,121,124,125,127]). However, some of the methods have good imperceptibility [113,114,120,122,123,125,127], focus on selecting the optimum strength factor [115] while some of them have robustness against geometric [113,116,119,122–126] and signal processing [113,116,120,122–126] attacks. Also, some of them were evaluated for combined attacks [116,119,121,124,125,127].

Point clouds: Table 9 shows that all but one of the watermarking methods developed for point cloud data are robust watermarking methods. Similarly to 3D image/video watermarking, there is a large research gap in the field of point cloud watermarking for fragile and semi-fragile watermarking. Table 10 shows that many approaches are vulnerable to cropping attacks [129–132] and have non-blindness [128,137]. One of them has a calculation burden [133], and two of them have drawbacks against noise attacks [134,138]. It is also seen from the table that some of the methods have good imperceptibility [128,129,134], no distortions [139] while some of them focus on the trade of robustness and imperceptibility [129,131] and have robustness against cropping attacks [134,137,138].

NeRF: While NeRF has gained significant attention in recent research, the exploration of NeRF watermarking remains limited due to its novelty. Table 9 highlights only eleven studies on NeRF watermarking [140–150], all classified under the robust category. This observation underscores the emerging stage of NeRF watermarking, indicating its current distance from maturity. To advance this field, there is a pressing need to expand the diversity of methodologies employed.

Summary: Table 3 and Fig. 6 reveals limited research in point cloud and deep learning-based 3D watermarking methods. Only eleven works [140–150] address NeRF watermarking. Conversely, Table 9 illustrates a scarcity of fragile and semi-fragile methods. Overall, the development of point cloud watermarking, NeRF watermarking, deep learning-based watermarking, and robust 3D mesh watermarking methods resistant to print-scan operations would invite further investigation and research attention.

8. Input and output

3D watermark techniques, in general, primarily involve embedding watermarks into a specific 3D representation, such as 3D meshes, depth images, videos, and point clouds. Notably, these methods often exhibit similarity between their input and output data, maintaining the essential characteristics of the original representation while incorporating the watermark for integrity and authenticity verification purposes.

Here, we specifically highlight and discuss some special cases of recent watermarking techniques [51,52,71,85,140–143,145–150]. These methods differ from others in terms of the extraction process, where the watermark is extracted from another type or version of the embedding process output, such as 2D renderings of 3D meshes or a printed 3D mesh version. These methods focus on addressing special types of problems like print-scan attacks. Consequently, the output of the embedding process differs from the input of the extraction process in these methods. Table 11 illustrates the embedding and extraction process of these special cases. In [51,52,71], unlike other 3D mesh watermarking methods, the watermark is extracted from printed 3D models after scanning. In [85], the watermark is embedded into the 3D mesh, while it is extracted from 2D renderings of 3D meshes.

Additionally, the watermark is extracted from 2D renderings of NeRF in [140–142,145–150], while [143] embeds the watermark into the NeRF model by fine-tuning and extracts the watermark from LL subbands of the NeRF rendered images.

9. Data sets

This section provides information about the data sets used in testing 3D watermarking methods. Table 12 displays the specific data sets employed for 3D watermarking. Many experiments on 3D meshes and point clouds have focused on a small selection of shapes like Bunny, Horse, Venus, and Armadillo. These shapes are commonly sourced from general data sets such as [161–163], and [164]. However, other data sets like A Large Dataset of Object Scans, which is a dataset of more than ten thousand 3D scans of real objects [165], 3D-FUTURE, which is the large-scale benchmark of 3D furniture shapes in the household scenario [166], OmniObject3D, which is a dataset of high-quality, real-scanned 3D objects with a large vocabulary [167], and CoMA, which is a dataset of extreme expressions captured over 12 different subjects [168] remain underutilized in 3D watermarking research. Similar trends are observed in 3D video and image watermarking, where evaluations typically rely on specific data sets or data points like datasets provided by the MEPG 3DAV group [169] and Visual Media Group of Microsoft Research [170], RMIT3DV, which is a creative commons uncompressed HD 3D video database [171], NAMA3DS1-COSPAD1, which is Subjective video quality assessment database [172], MSD, which is Middlebury stereo datasets [173] and etc [172,174–177]. Diversifying the data sets used for evaluation could enhance the effectiveness of assessing watermarking methods.

We have also included 4D data sets in this section to showcase new research paths for scholars. Table 12 displays both 3D and 4D data sets. In recent years, 4D technologies become increasingly important [185], necessitating methods for securing and sharing 4D data. Many public 4D data sets remain unexplored [181–184]. These public datasets offer research opportunities for developing 4D watermarking for research and industry. Certain 4D data sets encompass voice, image, and 3D mesh data [184], requiring diverse watermarking algorithms to ensure their security.

10. Metrics

Various metrics play essential roles in evaluating watermarking methods. These metrics, categorized as imperceptibility, robustness, and tamper detection, serve distinct purposes. Imperceptibility metrics gauge the quality of watermarked data, while robustness metrics assess method effectiveness against attacks. Some metrics, such as Peak Signal to Noise Ratio (PSNR) and Structural Similarity Index Measure (SSIM), serve both imperceptibility and robustness evaluation. PSNR focuses solely on pixel-wise differences, while SSIM considers structural information and human visual perception factors. Tamper detection metrics measure manipulation detection performance, either locally or globally. They determine the correctness rate of a method in correctly or falsely classifying tampered signals or parts of the signal. Table 13 classifies performance metrics by usage purpose and data type, elucidating their utilization across various studies.

Table 13 highlights the prevalent metrics used to evaluate 3D watermarking methods. For robustness assessment, Bit Error Rate (BER)

Table 11
Embedding and extraction process of the special cases.

Methods	Embedding process		Extracting process	
	Input	Output	Input	Output
[71], [51], [52]	3D mesh	Watermarked 3D mesh	Printed 3D mesh	Watermark
[85]	3D mesh	Watermarked 3D mesh	2D renderings of 3D meshes	Watermark
[140], [142], [146], [149], [150]	2D images	Watermarked NeRF model	NeRF-rendered images	Watermark
[143]	NeRF model	Watermarked NeRF model	LL subband of NeRF-rendered images	Watermark
[141], [145], [147], [148]	NeRF model	Watermarked NeRF model	NeRF-rendered images	Watermark

Table 12
Data sets for evaluating watermarking methods.

Data type	Data sets
3D mesh and point cloud	[161], [162], [163], [164], [165], [166], [167], [168]
3D video and image	[169], [170], [174], [171], [172], [175], [176], [177], [173]
NeRF	[178], [179], [180]
4D data	[181], [182], [183], [184]

and correlation are frequently employed, whereas PSNR and SSIM are prominent for evaluating the imperceptibility of 3D watermarked data. Correlation measures the similarity or association between two signals, while BER quantifies the accuracy by measuring the rate of bit errors. Specifically for 3D mesh watermarking, Maximum Root Mean Square Error (MRMS) and Mesh Structural Distortion Measure (MSDM) are commonly used imperceptibility metrics. MSDM measures the visual degradation, while MRMS calculates the surface-to-surface distance between watermarked and original meshes [161]. Some methods undergo subjective quality analysis, including Mean Opinion Score (MOS) for imperceptibility evaluation. MOS involves quantifying subjective impressions using a predefined quality scale by asking people [186]. Notably, metrics like PSNR and SSIM serve dual roles in assessing both imperceptibility and robustness. Table 13 also shows that while most watermarking methods are evaluated using a limited number of metrics, a few, such as those referenced in [77,78,115], are subjected to a more comprehensive evaluation framework. However, there is still a gap in tamper detection for 3D images and video. One of the reasons may be that 3D images and video watermarking are commonly employed for copyright enforcement. Fragile watermarking methods are designed to be highly sensitive to any modifications in the watermarked signal. However, 3D-rendered images are often subjected to various transformations during the rendering process, such as viewpoint changes or interpolation, which can introduce significant distortions. It is difficult for fragile watermark methods to survive these transformations.

11. Discussion and future research direction

In this section, we explore the challenges and future directions of 3D watermarking. We examine various 3D watermarking methods, their classification, the attacks they encounter, the metrics used for evaluation, and the datasets employed in experiments.

Challenges of 2D images/video watermarking vs 3D watermarking: Comparing 2D image/video watermarking with its 3D counterpart is crucial for understanding the unique challenges and opportunities each presents. While 2D watermarking is an established field, 3D watermarking faces greater complexity due to structural differences. While images consist of regular pixels, meshes contain vertices and face information. Pixels have value limitations (0–255), unlike mesh vertices. Operations like rotation, translation, and scaling can be performed on 3D objects without distorting their shape, posing challenges for watermarking. However, incorrect operations on 3D meshes may cause irreversible damage, complicating watermark removal. Moreover, while standards and tools for 2D images are abundant, those for 3D meshes are less common. Transformation space techniques in 3D watermarking are more limited, restricting the development of new methods. Despite these differences, lessons learned from 2D watermarking can contribute to the advancement of 3D techniques, offering valuable insights for future progress. For instance, techniques such as self-embedded watermarking for tamper detection and recovery [187], as well as the selection of embedding parameters through optimization algorithms [188], are examples of insights obtained from image watermarking that can be applied to the domain of 3D watermarking.

Challenges of 3D image/video vs 3D mesh/point cloud watermarking: Applying 3D image/video watermarking to 3D meshes is difficult due to differences in data structure, embedding methods, and robustness needs. 3D images/videos use structured pixel grids, while meshes consist of irregular vertices and faces, making direct adaptation challenging. Meshes also lack a fixed reference frame, so operations like remeshing or simplification can alter vertex connectivity. 3D mesh watermarking must resist content-preserving attacks such as rotation, translation, and scaling, which do not visually change the content. 3D image/video watermarking techniques lack these features, as they have different requirements specific to their domain. Another challenge is perceptibility: small pixel adjustments in 3D images/videos are often unnoticed, but vertex changes in meshes can cause visible distortions. Point cloud watermarking faces similar issues due to its unstructured nature.

3D mesh watermarking vs point cloud watermarking: A 3D mesh represents an object using a structured arrangement of vertices, edges, and faces, while a point cloud is an unstructured collection of points in 3D space, typically from 3D scans, without explicit connections. Topology-based 3D mesh watermarking methods, such as [73], are not applicable to point clouds due to the lack of connectivity. However, techniques like [41], which do not rely on faces or edges, can be applied to both 3D meshes and point clouds. Similarly, point cloud watermarking methods focused on point data can be used in 3D mesh watermarking.

Copyright protection of the printed 3D object: One of the primary challenges faced by 3D mesh watermarking methods is their resilience against print-scan attacks. As technology advances, it has become increasingly possible for digital 3D meshes created by the rightful owner to be replicated using 3D printers without permission and then used for commercial purposes. In our observations (see Table 10), the majority of existing methods lack robustness against such attacks, except for those discussed in [51,52,71]. The development of robust 3D mesh watermarking techniques capable of withstanding printing is still in its early stages and demands significant attention [35]. Moreover, the choice of devices used for 3D printing can significantly impact the robustness of these methods. The inclusion of a scanning process is essential; however, many methods omit this step, rendering them unevaluated against print-scan attacks. It is evident that the field requires further advancements in this regard.

Table 13
Performance metrics for evaluating 3D watermarking methods.

	Metric	3D Image	3D video	3D Mesh	Point cloud	NeRF
Robustness	Bit Error Rate (BER)	[127], [113], [114], [115], [116], [118], [119], [120], [121], [123], [124], [125], [126]	[108], [100], [101], [43], [102], [104], [96], [106], [107]	[92], [44], [48], [49], [93], [88], [94], [51], [56], [57], [91], [62], [82], [65], [67], [69]	[137], [128], [129], [134]	[142]
	Correlation	[115], [117], [122]	[97], [99], [100], [43], [103], [104], [105], [96], [106], [107]	[76], [78], [47], [48], [80], [71], [88], [89], [52], [54], [90], [55], [81], [56], [91], [59], [61], [82], [63], [64], [83], [68], [70], [72], [73], [74]	[128], [129], [130], [139], [131], [132], [135]	[142]
	Peak Signal to Noise Ratio (PSNR)	[117]		[76], [80]	[137]	[144], [150]
	Hamming distance	[120]				
	intra-BER		[110], [111], [112]			
	intra-NC		[109]			
	Bit Correction Rate (BCR)		[97]			
	False negative rate (FNR)		[98]			
	Bit Accuracy			[85], [86], [87], [75]		[140], [143], [145], [146], [148], [149]
	Structural similarity index measure (SSIM)			[50], [84]		[141], [144], [147], [150]
	Classification Accuracy					[141]
	Equal error rate (EER)			[88]	[130]	
	Match Percentage				[138]	
	Success rate			[51]		
	Message Error Rate (MER)			[53]		
	False positive rate (FPR)			[71]		
	Error Rate			[66]		
	Normalized mean squared error (NMSE)			[73]		
Imperceptibility	Peak Signal to Noise Ratio (PSNR)	[127], [113], [114], [115], [116], [118], [119], [120], [121], [122], [123], [124], [125], [126]	[109], [97], [98], [99], [100], [101], [43], [102], [103], [104], [105], [96], [106], [107]	[85], [76], [46], [53], [95], [57], [82], [83], [72], [74]	[137], [134], [135]	[140], [141], [142], [143], [144], [145], [147], [148], [149], [150]
	Structural similarity index measure (SSIM)	[127], [113], [114], [116], [118], [119], [120], [123], [124], [125], [126]	[109], [101], [43], [104]	[85], [53]		[140], [141], [142], [143], [144], [145], [147], [148], [149], [150]
	Feature similarity (FSIM)	[114]				
	Multi-scale SSIM (MS-SSIM)	[114], [115]				
	Mean opinion score (MOS)	[114]	[98], [102]	[78], [56]		
	Mean Square Error (MSE)	[115]		[53], [66]		
	Visual Information Fidelity, pixel domain version (VIFp)	[120]	[101]			
	Double stimulus continuous quality scale (DSCQS)	[123], [125]				

(*continued on next page*)

Table 13 (*continued*).

	Learned Perceptual Image Patch Similarity (LPIPS)			[140], [141], [142], [143], [144], [145], [147], [148], [149]
	Root Mean Square Error (RMSE)	[45], [46], [54], [63], [64], [74]	[137], [128], [129], [130], [139], [135]	[150]
	Signal-to-noise ratio (SNR)	[92], [93], [94], [52], [58], [66], [73]	[129], [130]	
	Change rate (CR)		[139]	
	Hausdorff distance	[45], [46], [78], [47], [86], [87], [55], [56], [58], [72], [74], [75]	[131], [133], [135]	
	The maximum movement distance (MaxD)	[92], [93], [94]		
	Average move distance (AvgD)	[92], [93], [94], [73]		
	Rate by User	[85]		
	Mean Square Quadratic Error (MSQE)	[76], [80], [82], [83]		
	Correlation distance	[77], [79], [50], [84]		
	Cosine distance	[77], [79], [50], [84]		
	Euclidean distance	[77], [79], [50], [84]		
	Manhattan distance	[77], [79], [50], [84]		
	Vertex Signal-to-Noise Ratio (VSNR)	[44], [45], [54], [57], [64]		
	Modified Hausdroff distance (MHD)	[45]		
	Maximum root mean square error (MRMS)	[78], [49], [51], [87], [55], [95], [81], [56], [58], [59], [61], [62], [70] [72]		
	Mesh structural distortion measure (MSDM)	[78], [49], [51], [95], [58], [61], [62], [67], [68]		
	Roughness	[47]		
	L1 Normal	[86]		
	MSDM2	[71], [63]		
	Normalized Absolute Error (NAE)	[53]		
	Normalized Hausdorff Distance (NHD)	[53]		
	Normalized root mean square error (NRMSE)	[53], [60]		
	Curvature consistency loss	[87]		
	Fast mesh perceptual distance (FPDM)	[58]		
	Average and maximum Distortion	[65]		
Tamper Detection	Accuracy (ACC)	[45]	[133], [136]	
	Number of vertices	[92], [93], [94], [60]		
	Precision rate (PPV)	[45]		
	Sensitivity rate (TPR)	[45]		
	Average False Rejection Rate (Avg. FRR)	[95]		

Optimal embedding strength factor: We have also identified an additional concern regarding the need to determine the optimal embedding strength factor to achieve a balance between robustness and imperceptibility during the watermark embedding process. Many 3D watermarking methods typically determine this factor intuitively, which may not be ideal considering its significant impact on method performance. Furthermore, intuitive determination of the strength factor limits the applicability of watermarking methods, as the optimal strength factor may vary for each 3D dataset and watermark [188]. In contrast, 2D image watermarking methods benefit from a toolbox of optimization algorithms such as the Artificial Bee Colony Algorithm, Particle Swarm Optimization, Grey Wolf Optimizer, etc., which have proven successful [189]. Hence, integrating optimization techniques stands out as a viable avenue for enhancing 3D watermarking methods that utilize embedding strength.

Tamper detection and recovery: When examining 3D watermarking methods, it becomes evident that numerous researchers prioritize robust watermarking. Especially within the realms of 3D image and video watermarking, it poses a significant challenge for fragile watermarks to endure the 3D-rendering process, which subjects them to various transformations. While ownership verification is crucial, detecting forgeries in 3D data and identifying tampered areas are equally significant. Developing novel fragile and semi-fragile methods presents a promising research avenue. In addition to detecting tampered regions, the ability to recover tampered areas could prove invaluable across various fields reliant on 3D data. Recent advancements in 2D image watermarking have shown significant success [187,190,191]. Learning and adapting from self-embedded watermarking mechanisms to 3D watermarking could be a potential direction for future research.

Deep learning-based watermarking and NeRF watermarking: Table 3 reveals a scarcity of both deep learning-based approaches and those tailored for NeRF. Deep learning methods, which have demonstrated significant success across various domains [192,193], exhibit potential over classical watermarking techniques due to their superior performance in many fields. Consequently, there is a growing trend towards prioritizing the development of deep learning-based 3D watermarking methods. Moreover, with NeRF emerging as a recent and important medium for scene representation, researchers must stay updated on evolving NeRF technologies and ensure their security. For instance, the NOFA framework [194] allows for the creation of highly detailed facial avatars using just one image, posing a potential risk of misuse by malicious actors. Thus, tools are needed to verify the authenticity of avatars created with this framework and secure synthesized videos with watermarking [194]. Given the limited number of methods available for NeRF watermarking, more attention can be allocated to this new area. Concurrently, ongoing studies focusing on 3D mesh production using NeRF technology underscore the importance of securing NeRF models intended for such production to safeguard ownership rights.

Dynamic mesh and point cloud watermarking: While conducting the survey, we observed that only two techniques target dynamic mesh and point cloud watermarking [151,195]. Both assume that the change of each vertex on the time axis must be known. However, it is not possible to apply these methods to 4D data that lacks a fixed number of vertices and whose trajectories are unknown. In [151], frame averaging attacks were used as a temporal synchronization attack. Specifically, one frame was deleted for each 24, 12, and 6 frames, and then the average of the two adjacent frames was placed instead of the deleted frame. However, this method was only evaluated against one temporal attack and not against others such as frame deletion and displacement. Since the watermarks are embedded in the transform coefficient of the vertex along the time axis in this method, it is considered vulnerable to frame deletion attacks. On the other hand, another method [195] proposed for dynamic 3D mesh watermarking has not been evaluated against temporal synchronization attacks.

Our observation highlights a notable absence of watermarking techniques designed for dynamic 3D mesh and point cloud data that incorporate temporal information. Simply preserving ownership of individual meshes within 4D datasets is insufficient, as sequence information is equally vital. Therefore, it is imperative for researchers to prioritize the development of watermarking techniques specifically tailored to dynamic 3D mesh and point cloud data, as this will significantly enhance 4D watermarking capabilities.

Evaluation of the methods against attacks: Various types of attacks are commonly used to assess watermarking methods. However, the utilization of combined attacks in method evaluations remains limited, despite the potential for multiple operations on data. Robustness against combined attacks is crucial for ensuring the effectiveness and applicability of methods. Particularly, print-scan attacks, as mentioned earlier, should also be incorporated as one component of combined attacks. In the emerging field of NeRF watermarking, a comprehensive range of attacks, including image manipulations, should be employed for thorough evaluation, given that many image manipulations can be applied to the 2D image renderings of NeRF. Model-based attacks, such as weight alterations, adversarial attacks, and modification of only the watermarking component, are essential for assessing deep learning and NeRF watermarking methods. Additionally, many 3D methods are susceptible to cropping attacks, which can significantly compromise shape integrity. Successfully countering cropping attacks enhances method reliability.

Usage of metrics: Table 13 demonstrates that many methods use a limited number of metrics for evaluation. The choice of metrics can significantly impact method performance, highlighting the need for diverse metrics to provide a comprehensive assessment. While objective analysis predominates in research, it is also important to consider visual perception for subjective evaluation. Incorporating visual quality assessment, as advocated by [56], enhances result reliability. In evaluating 3D video watermarking methods, metrics must encompass the entire video rather than assessing individual frames alone. Similarly, for 4D and dynamic mesh watermarking, evaluating the complete 4D dataset or sequence of 3D meshes provides a more holistic perspective on method effectiveness.

Data sets: Our observations also indicate that 3D watermarking methods are typically evaluated on a limited dataset, often using standard meshes such as Bunny and Venus. However, method evaluations should encompass diverse datasets with varying characteristics to uncover unknown strengths and weaknesses. Experimenting with large, complex datasets enhances our understanding of method performance, especially considering the availability of extensive public 3D datasets like A Large Dataset of Object Scans [165] and OmniObject3D [167]. With the increasing prevalence of 4D datasets across various domains, researchers should explore 4D watermarking techniques to safeguard these datasets. The abundance of 4D datasets, including audio data, such as HUMAN4D [184], presents opportunities for developing novel watermarking methods tailored to the security requirements of 4D data.

Technique Diversification: It is crucial to encourage the community to explore a diverse range of techniques in watermarking processes. This diversification expands the array of available watermarking options, making them less vulnerable to attacks and more challenging to compromise. Additionally, releasing the source code for implementation and comparison facilitates transparency and reproducibility in research, fostering collaboration and advancement in the field.

12. Conclusion

This survey comprehensively explores various aspects of 3D watermarking, including different types of 3D methods, their categorization, technical idea breakdown, and methodological evaluations. It outlines attacks based on data type and metrics used for evaluation, including both standard and underutilized datasets for experimentation.

Moreover, the survey aims to guide researchers towards future directions in 3D watermarking, such as optimizing strength factors, protecting copyrights for 3D printed objects, and addressing challenges like tamper detection and recovery, 4D, and NeRF watermarking. These areas hold significant potential for both academic and industrial communities.

To enhance method effectiveness, we recommend further attention should be given to cropping, combined, and print-scan attacks, alongside incorporating comprehensive objective and subjective analyses during evaluation. It is important for further research in 3D watermarking to strike a balance between imperceptibility, robustness, and capacity. These remain crucial for practical applications leveraging 3D technologies.

CRediT authorship contribution statement

Ertugrul Gul: Writing – review & editing, Writing – original draft, Methodology, Investigation, Funding acquisition, Conceptualization. **Gary K.L. Tam:** Writing – review & editing, Conceptualization.

Declaration of competing interest

The authors declare the following financial interests/personal relationships which may be considered as potential competing interests: Ertugrul Gul reports financial support and travel were provided by Scientific and Technological Research Council of Turkey. Gary Tam reports travel was provided by The Royal Society. Gary Tam reports a relationship with Swansea University that includes: employment. Ertugrul Gul reports a relationship with Kayseri University that includes: employment.

Acknowledgments

This study received support from the Scientific and Technical Research Council of Turkey (TUBITAK) under the 2219 postdoctoral fellowship support program, project number 1059B192202811. Tam acknowledges partial support from a Royal Society fund (IEC/NSFC/21 1159). Additionally, the study received partial visiting researcher support from the Faculty of Engineering at Swansea University. The authors express gratitude to TUBITAK, Kayseri University, and Swansea University for their support. For the purpose of Open Access, the author has applied a Creative Commons Attribution (CC BY) license to any Author Accepted Manuscript (AAM) version arising from this submission.

Data availability

No data was used for the research described in the article.

References

[1] E. Gul, S. Ozturk, A secret image sharing method based on block-wise cheating detection and recovery on shadow images, Comput. Electr. Eng. 110 (2023) 108882.
[2] T. Luo, Y. Zhou, Z. He, G. Jiang, H. Xu, S. Qi, Y. Zhang, Stegmamba: Distortion-free immune-cover for multi-image steganography with state space model, IEEE Trans. Circuits Syst. Video Technol. (2024).
[3] M.T. Ahvanooey, Q. Li, X. Zhu, M. Alazab, J. Zhang, ANiTW: A novel intelligent text watermarking technique for forensic identification of spurious information on social media, Comput. Secur. 90 (2020) 101702.
[4] T. Saba, M. Bashardoost, H. Kolivand, M.S.M. Rahim, A. Rehman, M.A. Khan, Enhancing fragility of zero-based text watermarking utilizing effective characters list, Multimedia Tools Appl. 79 (2020) 341–354.
[5] X.-C. Yuan, C.-M. Pun, C.P. Chen, Robust mel-frequency cepstral coefficients feature detection and dual-tree complex wavelet transform for digital audio watermarking, Inform. Sci. 298 (2015) 159–179.
[6] M. Yamni, H. Karmouni, M. Sayyouri, H. Qjidaa, Robust audio watermarking scheme based on fractional charlier moment transform and dual tree complex wavelet transform, Expert Syst. Appl. 203 (2022) 117325.
[7] E. Gul, A blind robust color image watermarking method based on discrete wavelet transform and discrete cosine transform using grayscale watermark image, Concurr. Comput.: Pr. Exp. 34 (22) (2022) e6884.
[8] G. Azizoğlu, A.N. Toprak, A QR code-based robust color image watermarking technique, in: The International Conference on Artificial Intelligence and Applied Mathematics in Engineering, Springer, 2022, pp. 445–457.
[9] T. Luo, J. Wu, Z. He, H. Xu, G. Jiang, C.-C. Chang, Wformer: A transformer-based soft fusion model for robust image watermarking, IEEE Trans. Emerg. Top. Comput. Intell. 8 (6) (2024) 4179–4196.
[10] H. Prasetyo, C.-H. Hsia, C.-H. Liu, Vulnerability attacks of SVD-based video watermarking scheme in an IoT environment, IEEE Access 8 (2020) 69919–69936.
[11] E. Farri, P. Ayubi, A robust digital video watermarking based on CT-SVD domain and chaotic DNA sequences for copyright protection, J. Ambient. Intell. Humaniz. Comput. 14 (10) (2023) 13113–13137.
[12] M. Asikuzzaman, M.R. Pickering, An overview of digital video watermarking, IEEE Trans. Circuits Syst. Video Technol. 28 (9) (2017) 2131–2153.
[13] A.K. Singh, Data hiding: current trends, innovation and potential challenges, ACM Trans. Multimed. Comput. Commun. Appl. (TOMM) 16 (3s) (2020) 1–16.
[14] A. Anand, A.K. Singh, Watermarking techniques for medical data authentication: a survey, Multimedia Tools Appl. 80 (2021) 30165–30197.
[15] L. Tanwar, J. Panda, Hybrid reversible watermarking algorithm using histogram shifting and pairwise prediction error expansion, Multimedia Tools Appl. (2023) 1–23.
[16] G. Azizoglu, A.N. Toprak, A novel reversible fragile watermarking method in DWT domain for tamper localization and digital image authentication, Biomed. Signal Process. Control. 84 (2023) 105015.
[17] S.P. Mohanty, E. Kougianos, Real-time perceptual watermarking architectures for video broadcasting, J. Syst. Softw. 84 (5) (2011) 724–738.
[18] N. Ren, X. Pang, C. Zhu, S. Guo, Y. Xiong, Blind and robust watermarking algorithm for remote sensing images resistant to geometric attacks, Photogramm. Eng. Remote Sens. 89 (5) (2023) 60–71.
[19] M. Kumar, J. Aggarwal, A. Rani, T. Stephan, A. Shankar, S. Mirjalili, Secure video communication using firefly optimization and visual cryptography, Artif. Intell. Rev. (2022) 1–21.
[20] P. Garg, A. Jain, A robust technique for biometric image authentication using invisible watermarking, Multimedia Tools Appl. 82 (2) (2023) 2237–2253.
[21] O.F. Saritas, S. Ozturk, A blind CT and DCT based robust color image watermarking method, Multimedia Tools Appl. 82 (10) (2023) 15475–15491.
[22] O.F. Saritas, S. Ozturk, A color channel multiplexing approach for robust discrete wavelet transform based image watermarking, Concurr. Comput.: Pr. Exp. 34 (25) (2022) e7255.
[23] K. Wang, S. Wu, X. Yin, W. Lu, X. Luo, R. Yang, Robust image watermarking with synchronization using template enhanced-extracted network, IEEE Trans. Circuits Syst. Video Technol. (2024).
[24] B. Yang, G. Lim, J. Hur, Toward practical deep blind watermarking for traitor tracing, IEEE Access 11 (2023) 72836–72847.
[25] G. Wang, Z. Ma, C. Liu, X. Yang, H. Fang, W. Zhang, N. Yu, Must: Robust image watermarking for multi-source tracing, in: Proceedings of the AAAI Conference on Artificial Intelligence, vol. 38, (6) 2024, pp. 5364–5371.
[26] T. Kalker, G. Depovere, J. Haitsma, M.J. Maes, Video watermarking system for broadcast monitoring, in: Security and Watermarking of Multimedia Contents, vol. 3657, SPIE, 1999, pp. 103–112.
[27] K. Thaiyalnayaki, R. Dhanalakshmi, A chaos encrypted video watermarking scheme for the enforcement of playback control, Int. J. Adv. Eng. Technol. 4 (1) (2012) 165.
[28] F.N. Thakkar, V.K. Srivastava, A fast watermarking algorithm with enhanced security using compressive sensing and principle components and its performance analysis against a set of standard attacks, Multimedia Tools Appl. 76 (2017) 15191–15219.
[29] A.K. Sahu, M. Hassaballah, R.S. Rao, G. Suresh, Logistic-map based fragile image watermarking scheme for tamper detection and localization, Multimedia Tools Appl. 82 (16) (2023) 24069–24100.
[30] E. Gul, S. Ozturk, A novel hash function based fragile watermarking method for image integrity, Multimedia Tools Appl. 78 (2019) 17701–17718.
[31] M. Narendra, M. Valarmathi, L.J. Anbarasi, Watermarking techniques for three-dimensional (3D) mesh models: a survey, Multimedia Syst. (2022) 1–19.
[32] W. Wan, J. Wang, Y. Zhang, J. Li, H. Yu, J. Sun, A comprehensive survey on robust image watermarking, Neurocomputing 488 (2022) 226–247.
[33] D. Dhaou, S. Ben Jabra, E. Zagrouba, A review on anaglyph 3D image and video watermarking, 3D Res. 10 (2019) 1–12.
[34] S. Borah, B. Borah, Watermarking techniques for three dimensional (3D) mesh authentication in spatial domain, 3D Res. 9 (2018) 1–22.
[35] J.-U. Hou, D. Kim, W.-H. Ahn, H.-K. Lee, Copyright protections of digital content in the age of 3d printer: Emerging issues and survey, IEEE Access 6 (2018) 44082–44093.
[36] B. Mildenhall, P.P. Srinivasan, M. Tancik, J.T. Barron, R. Ramamoorthi, R. Ng, Nerf: Representing scenes as neural radiance fields for view synthesis, Commun. ACM 65 (1) (2021) 99–106.

[37] B.H. Kumar, H. Chennamma, Watermarking of computer generated imagery: A review, in: 2019 IEEE International Conference on Electrical, Computer and Communication Technologies, ICECCT, IEEE, 2019, pp. 1–7.
[38] D. Mukherjee, S. Mukhopadhyay, Hardware efficient architecture for 2D DCT and IDCT using taylor-series expansion of trigonometric functions, IEEE Trans. Circuits Syst. Video Technol. 30 (8) (2019) 2723–2735.
[39] J.-M. Guo, H. Prasetyo, False-positive-free SVD-based image watermarking, J. Vis. Commun. Image Represent. 25 (5) (2014) 1149–1163.
[40] K.K. Jabbar, M.B. Tuieb, S.A. Thajeel, Digital watermarking by utilizing the properties of self-organization map based on least significant bit and most significant bit, Int. J. Electr. Comput. Engineering (IJECE) 12 (6) (2022) 6545–6558.
[41] J.-W. Cho, R. Prost, H.-Y. Jung, An oblivious watermarking for 3-D polygonal meshes using distribution of vertex norms, IEEE Trans. Signal Process. 55 (1) (2006) 142–155.
[42] M. Mazziotta, A. Pareto, Normalization methods for spatio-temporal analysis of environmental performance: Revisiting the min–max method, Environmetrics 33 (5) (2022) e2730.
[43] S.B. Jabra, E. Zagrouba, M.B. Farah, A new efficient anaglyph 3D image and video watermarking technique minimizing generation deficiencies, Multimedia Tools Appl. 83 (7) (2024) 19433–19463.
[44] R. Jin, J. Kim, Coordinate quantization transformation citygml watermarking, Multimedia Tools Appl. 81 (6) (2022) 8561–8573.
[45] K. Mamdouh, N.A. Semary, H. Ahmed, A blind fragile watermarking for 3D triangular model based on curvature features and chaos sequence, IJCI. Int. J. Comput. Inf. 9 (2) (2022) 14–24.
[46] M. Narendra, M. Valarmathi, L.J. Anbarasi, M.V.R. Sarobin, F. Al-Turjman, High embedding capacity in 3D model using intelligent fuzzy based clustering, Neural Comput. Appl. 34 (20) (2022) 17783–17792.
[47] N. Medimegh, S. Belaid, M. Atri, N. Werghi, 3D mesh watermarking using salient points, Multimedia Tools Appl. 77 (2018) 32287–32309.
[48] S. Ren, H. Cheng, A. Fan, Dual information hiding algorithm based on the regularity of 3D mesh model, Optoelectron. Lett. 18 (9) (2022) 559–565.
[49] H.-U. Jang, H.-Y. Choi, J. Son, D. Kim, J.-U. Hou, S. Choi, H.-K. Lee, Cropping-resilient 3D mesh watermarking based on consistent segmentation and mesh steganalysis, Multimedia Tools Appl. 77 (2018) 5685–5712.
[50] H.S. Al-Saadi, A. Elhadad, A. Ghareeb, et al., Rapid and blind watermarking approach of the 3D objects using QR code images for securing copyright, Comput. Intell. Neurosci. 2021 (2021).
[51] A. Delmotte, K. Tanaka, H. Kubo, T. Funatomi, Y. Mukaigawa, Blind 3D-printing watermarking using moment alignment and surface norm distribution, IEEE Trans. Multimed. 23 (2020) 3467–3482.
[52] Y. Chen, Z. Ma, H. Zhou, W. Zhang, 3D print-scan resilient localized mesh watermarking, in: 2021 IEEE International Workshop on Information Forensics and Security, WIFS, IEEE, 2021, pp. 1–6.
[53] G. Mostafa, W. Alexan, A robust high capacity gray code-based double layer security scheme for secure data embedding in 3d objects, Int. J. Comput. Digit. Syst. 10 (2020) 1–9.
[54] N. Sharma, J. Panda, Statistical watermarking approach for 3D mesh using local curvature estimation, IET Inf. Secur. 14 (6) (2020) 745–753.
[55] N. Medimegh, S. Belaid, M. Atri, N. Werghi, Statistical 3D watermarking algorithm using non negative matrix factorization, Multimedia Tools Appl. 79 (2020) 25889–25904.
[56] P. Singh, K.J. Devi, Blind, secured and robust watermarking for 3-D polygon mesh using vertex curvature, Int. J. Adv. Comput. Sci. Appl. 12 (8) (2021).
[57] R. ARTHY, K. Mala, et al., Hypothesis-based vertex shift method for embedding secret logos in the geometric features of 3D objects, Turk. J. Electr. Eng. Comput. Sci. 27 (6) (2019) 4518–4529.
[58] S. Borah, B. Borah, A blind, semi-fragile 3d mesh watermarking algorithm using minimum distortion angle quantization index modulation (3d-mdaqim), Arab. J. Sci. Eng. 44 (4) (2019) 3867–3882.
[59] L. Li, H. Li, W. Yuan, J. Lu, X. Feng, C.-C. Chang, A watermarking mechanism with high capacity for three-dimensional mesh objects using integer planning, IEEE Multimedia 25 (3) (2018) 49–64.
[60] Y.-Y. Tsai, Y.-S. Tsai, C.-C. Chang, An effective authentication algorithm for polygonal models with high embedding capacity, Symmetry 10 (7) (2018) 290.
[61] J. Liu, Y. Wang, Y. Li, R. Liu, J. Chen, A robust and blind 3D watermarking algorithm using multiresolution adaptive parameterization of surface, Neurocomputing 237 (2017) 304–315.
[62] H.-Y. Choi, H.-U. Jang, J. Son, H.-K. Lee, Blind 3D mesh watermarking based on cropping-resilient synchronization, Multimedia Tools Appl. 76 (2017) 26695–26721.
[63] Y. Yang, R. Pintus, H. Rushmeier, I. Ivrissimtzis, A 3D steganalytic algorithm and steganalysis-resistant watermarking, IEEE Trans. Vis. Comput. Graphics 23 (2) (2016) 1002–1013.
[64] O.M. El Zein, L.M. El Bakrawy, N.I. Ghali, A robust 3D mesh watermarking algorithm utilizing fuzzy C-means clustering, Futur. Comput. Informat. J. 2 (2) (2017) 148–156.
[65] A.M. Molaei, H. Ebrahimnezhad, M.H. Sedaaghi, Robust and blind 3D mesh watermarking in spatial domain based on faces categorization and sorting, 3D Res. 7 (2016) 1–18.
[66] H.-K. Chen, W.-S. Chen, GPU-accelerated blind and robust 3D mesh watermarking by geometry image, Multimedia Tools Appl. 75 (2016) 10077–10096.
[67] X. Rolland-Neviere, G. Doërr, P. Alliez, Triangle surface mesh watermarking based on a constrained optimization framework, IEEE Trans. Inf. Forensics Secur. 9 (9) (2014) 1491–1501.
[68] X. Feng, W. Zhang, Y. Liu, Double watermarks of 3D mesh model based on feature segmentation and redundancy information, Multimedia Tools Appl. 68 (2014) 497–515.
[69] R. Hu, L. Xie, H. Yu, B. Ding, et al., Applying 3D polygonal mesh watermarking for transmission security protection through sensor networks, Math. Probl. Eng. 2014 (2014).
[70] Y.-z. Zhan, Y.-t. Li, X.-y. Wang, Y. Qian, A blind watermarking algorithm for 3D mesh models based on vertex curvature, J. Zhejiang Univ. SCIENCE C 15 (5) (2014) 351–362.
[71] J.-U. Hou, D.-G. Kim, H.-K. Lee, Blind 3D mesh watermarking for 3D printed model by analyzing layering artifact, IEEE Trans. Inf. Forensics Secur. 12 (11) (2017) 2712–2725.
[72] J. Hu, M. Dai, X. Wang, Q. Xie, D. Zhang, Robust 3D watermarking with high imperceptibility based on EMD on surfaces, Vis. Comput. 40 (11) (2024) 7685–7700.
[73] L. Vandenberghe, C. Joslin, 3D model watermarking using surface integrals of generated random vector fields, Multimedia Syst. 30 (5) (2024) 253.
[74] R. Nan, L. Zhang, Y. Jin, J. Xie, S. Liu, H. Wang, Robust watermarking algorithm for oblique photography 3D models based on multi-level curvature and weighted distance, Earth Sci. Informatics 18 (3) (2025) 321.
[75] G. Hou, B. Ou, F. Peng, M. Long, A traitor tracing and access control method for encrypted 3D models based on CP-ABE and fair watermark, IEEE Signal Process. Lett. (2024).
[76] M. Jallouli, I. Sayahi, A.B. Mabrouk, Robust crypto-watermarking approach based on spherical harmonics and AES algorithm for 3D mesh safe transmission, Multimedia Tools Appl. 81 (27) (2022) 38543–38567.
[77] H. Abulkasim, M. Jamjoom, S. Abbas, Securing copyright using 3D objects blind watermarking scheme, Comput. Mater. Contin. 72 (3) (2022).
[78] M. Hamidi, A. Chetouani, M. El Haziti, M. El Hassouni, H. Cherifi, Blind robust 3D mesh watermarking based on mesh saliency and wavelet transform for copyright protection, Information 10 (2) (2019) 67.
[79] H.S. Al-Saadi, A. Ghareeb, A. Elhadad, et al., A blind watermarking model of the 3D object and the polygonal mesh objects for securing copyright, Comput. Intell. Neurosci. 2021 (2021).
[80] I. Sayahi, M. Jallouli, A.B. Mabrouk, M.A. Mahjoub, C.B. Amar, Robust hybrid watermarking approach for 3D multiresolution meshes based on spherical harmonics and wavelet transform, Multimedia Tools Appl. (2023) 1–26.
[81] S. Hachicha, I. Sayahi, A. Elkefi, C.B. Amar, M. Zaied, GPU-based blind watermarking scheme for 3D multiresolution meshes using unlifted butterfly wavelet transformation, Circuits Systems Signal Process. 39 (3) (2020) 1533–1560.
[82] I. Sayahi, A. Elkefi, C.B. Amar, Blind watermarking algorithm based on spiral scanning method and error-correcting codes, Multimedia Tools Appl. 76 (2017) 16439–16462.
[83] I. Sayahi, A. Elkefi, M. Koubaa, C.B. Amar, Robust watermarking algorithm for 3D multiresolution meshes, in: VISAPP (3), 2015, pp. 150–157.
[84] S.M. Alhammad, N. Ahmed, S. Abbas, H. Abulkasim, A. Elhadad, Robust 3D object watermarking scheme using shape features for copyright protection, PeerJ Comput. Sci. 10 (2024) e2020.
[85] I. Yoo, H. Chang, X. Luo, O. Stava, C. Liu, P. Milanfar, F. Yang, Deep 3d-to-2d watermarking: embedding messages in 3d meshes and extracting them from 2d renderings, in: Proceedings of the IEEE/CVF Conference on Computer Vision and Pattern Recognition, 2022, pp. 10031–10040.
[86] X. Zhu, G. Ye, X. Luo, X. Wei, Rethinking mesh watermark: Towards highly robust and adaptable deep 3D mesh watermarking, in: Proceedings of the AAAI Conference on Artificial Intelligence, vol. 38, (7) 2024, pp. 7784–7792.
[87] F. Wang, H. Zhou, H. Fang, W. Zhang, N. Yu, Deep 3D mesh watermarking with self-adaptive robustness, Cybersecurity 5 (1) (2022) 1–14.
[88] G. Liu, Q. Wang, L. Wu, R. Pan, B. Wan, Y. Tian, Zero-watermarking method for resisting rotation attacks in 3D models, Neurocomputing 421 (2021) 39–50.
[89] J.-S. Lee, Y.-C. Chen, C.-J. Chew, W.-C. Hung, Y.-Y. Fan, B. Li, Constructing gene features for robust 3D mesh zero-watermarking, J. Inf. Secur. Appl. 73 (2023) 103414.
[90] J.-S. Lee, C. Liu, Y.-C. Chen, W.-C. Hung, B. Li, Robust 3D mesh zero-watermarking based on spherical coordinate and skewness measurement, Multimedia Tools Appl. 80 (17) (2021) 25757–25772.
[91] X. Wang, Y. Zhan, A zero-watermarking scheme for three-dimensional mesh models based on multi-features, Multimedia Tools Appl. 78 (2019) 27001–27028.
[92] F. Peng, T. Liao, M. Long, J. Li, W. Zhang, Y. Zhou, Semi-fragile reversible watermarking for 3D models using spherical crown volume division, IEEE Trans. Circuits Syst. Video Technol. (2023).
[93] F. Peng, T. Liao, M. Long, A semi-fragile reversible watermarking for authenticating 3d models in dual domains based on variable direction double modulation, IEEE Trans. Circuits Syst. Video Technol. 32 (12) (2022) 8394–8408.

[94] F. Peng, B. Long, M. Long, A semi-fragile reversible watermarking for authenticating 3D models based on virtual polygon projection and double modulation strategy, IEEE Trans. Multimed. (2021).
[95] S. Borah, B. Borah, Prediction error expansion (PEE) based reversible polygon mesh watermarking scheme for regional tamper localization, Multimedia Tools Appl. 79 (17–18) (2020) 11437–11458.
[96] D. Dhaou, S. Ben Jabra, E. Zagrouba, An efficient anaglyph 3d video watermarking approach based on hybrid insertion, in: Computer Analysis of Images and Patterns: 18th International Conference, CAIP 2019, Salerno, Italy, September 3–5, 2019, Proceedings, Part II 18, Springer, 2019, pp. 96–107.
[97] K. Abdelhedi, F. Chaabane, W. Puech, C.B. Amar, A novel robust spread spectrum watermarking scheme for 3D video traitor tracing, IEEE Access (2023).
[98] M. Asikuzzaman, M.J. Alam, A.J. Lambert, M.R. Pickering, Robust DT CWT-based DIBR 3D video watermarking using chrominance embedding, IEEE Trans. Multimed. 18 (9) (2016) 1733–1748.
[99] E. El-Bakary, W. El-Shafai, S. El-Rabaie, O. Zahran, M. El-Halawany, F.A. El-Samie, Efficient secure optical DWT-based watermarked 3D video transmission over MC-CDMA wireless channel, J. Opt. (2023) 1–22.
[100] D. Dhaou, S. Ben Jabra, E. Zagrouba, A multi-sprite based anaglyph 3d video watermarking approach robust against collusion, 3D Res. 10 (2019) 1–15.
[101] S. Rana, 3D video watermarking for MVD based view-synthesis and RST attack, Multimedia Tools Appl. 83 (9) (2024) 26775–26795.
[102] Y. Luo, D. Peng, A robust digital watermarking method for depth-image-based rendering 3D video, Multimedia Tools Appl. 80 (2021) 14915–14939.
[103] W. El-Shafai, S. El-Rabaie, M. El-Halawany, F.A. El-Samie, Security of 3D-HEVC transmission based on fusion and watermarking techniques, Multimedia Tools Appl. 78 (2019) 27211–27244.
[104] S. Ben Jabra, E. Zagrouba, Robust anaglyph 3D video watermarking based on cyan mosaic generation and DCT insertion in krawtchouk moments, Vis. Comput. 38 (11) (2022) 3611–3625.
[105] W. El-Shafai, S. El-Rabaie, M. El-Halawany, F.E. Abd El-Samie, Efficient hybrid watermarking schemes for robust and secure 3D-mvc communication, Int. J. Commun. Syst. 31 (4) (2018) e3478.
[106] D. Dhaou, S.B. Jabra, E. Zagrouba, A robust anaglyph 3D video watermarking based on multi-sprite generation, in: ICETE (2), 2019, pp. 260–267.
[107] D. Dhaou, S.B. Jabra, E. Zagrouba, An efficient group of pictures decomposition based watermarking for anaglyph 3D video, in: VISIGRAPP (4: VISAPP), 2018, pp. 501–510.
[108] X. Liu, Y. Wang, Z. Sun, L. Wang, R. Zhao, Y. Zhu, B. Zou, Y. Zhao, H. Fang, Robust and discriminative zero-watermark scheme based on invariant features and similarity-based retrieval to protect large-scale DIBR 3D videos, Inform. Sci. 542 (2021) 263–285.
[109] X. Liu, R. Zhao, F. Li, S. Liao, Y. Ding, B. Zou, Novel robust zero-watermarking scheme for digital rights management of 3D videos, Signal Process., Image Commun. 54 (2017) 140–151.
[110] X. Liu, Y. Zhang, J. Wang, Y. Sun, W. Zhang, D. Zhou, G. Schaefer, H. Fang, Multiple-feature-based zero-watermarking for robust and discriminative copyright protection of DIBR 3D videos, Inform. Sci. 604 (2022) 97–114.
[111] X. Liu, Y. Zhang, S. Du, J. Zhang, M. Jiang, H. Fang, Discriminative and geometrically robust zero-watermarking scheme for protecting DIBR 3D videos, in: 2021 IEEE International Conference on Multimedia and Expo, ICME, IEEE, 2021, pp. 1–6.
[112] X. Liu, Y. Zhang, S. Du, J. Zhang, M. Jiang, H. Fang, DIBR zero-watermarking based on invariant feature and geometric rectification, IEEE MultiMedia 29 (3) (2022) 27–37.
[113] W.-H. Kim, J.-U. Hou, H.-U. Jang, H.-K. Lee, Robust template-based watermarking for DIBR 3D images, Appl. Sci. 8 (6) (2018) 911.
[114] S.-H. Nam, S.-M. Mun, W. Ahn, D. Kim, I.-J. Yu, W.-H. Kim, H.-K. Lee, NSCT-based robust and perceptual watermarking for DIBR 3D images, IEEE Access 8 (2020) 93760–93781.
[115] S. Koley, Bat optimized 3D anaglyph image watermarking based on maximum noise fraction in the digital shearlet domain, Multimedia Tools Appl. 81 (14) (2022) 19491–19523.
[116] W. Etoom, A. Al-Haj, A robust and imperceptible watermarking method for 3D DIBR images, Multimedia Tools Appl. 81 (20) (2022) 28165–28182.
[117] X. Zhang, W. Zhang, W. Sun, X. Sun, S.K. Jha, A robust 3-D medical watermarking based on wavelet transform for data protection., Comput. Syst. Sci. Eng. 41 (3) (2022).
[118] S. Wang, C. Cui, X. Niu, Watermarking for DIBR 3D images based on SIFT feature points, Measurement 48 (2014) 54–62.
[119] C. Cui, X.-M. Niu, A robust DIBR 3D image watermarking algorithm based on histogram shape, Measurement 92 (2016) 130–143.
[120] S. Rana, A. Sur, Depth-based view-invariant blind 3D image watermarking, ACM Trans. Multimed. Comput. Commun. Appl. (TOMM) 12 (4) (2016) 1–23.
[121] Y.-H. Lin, J.-L. Wu, A digital blind watermarking for depth-image-based rendering 3D images, IEEE Trans. Broadcast. 57 (2) (2011) 602–611.
[122] H.S. Devi, T. Imphal, K.M. Singh, A robust and optimized 3D red-cyan anaglyph blind image watermarking in the DWT domain, Contemp. Eng. Sci. 9 (32) (2016) 1575–1589.
[123] H.-D. Kim, J.-W. Lee, T.-W. Oh, H.-K. Lee, Robust DT-CWT watermarking for DIBR 3D images, IEEE Trans. Broadcast. 58 (4) (2012) 533–543.
[124] C. Cui, S. Wang, X. Niu, A novel watermarking for DIBR 3D images with geometric rectification based on feature points, Multimedia Tools Appl. 76 (2017) 649–677.
[125] S.-H. Nam, W.-H. Kim, S.-M. Mun, J.-U. Hou, S. Choi, H.-K. Lee, A SIFT features based blind watermarking for DIBR 3D images, Multimedia Tools Appl. 77 (2018) 7811–7850.
[126] A. Al-Haj, M.E. Farfoura, A. Mohammad, Transform-based watermarking of 3D depth-image-based-rendering images, Measurement 95 (2017) 405–417.
[127] Z. He, L. He, H. Xu, T.-Y. Chai, T. Luo, A bilateral attention based generative adversarial network for DIBR 3D image watermarking, J. Vis. Commun. Image Represent. 92 (2023) 103794.
[128] J. Liu, Y. Yang, D. Ma, Y. Wang, Z. Pan, A watermarking algorithm for 3D point cloud models using ring distribution, Trans. Edutainment XIV (2018) 56–68.
[129] J. Liu, Y. Yang, D. Ma, Y. Wang, Z. Pan, A watermarking method for 3D models based on feature vertex localization, IEEE Access 6 (2018) 56122–56134.
[130] J. Liu, Y. Yang, D. Ma, W. He, Y. Wang, A novel watermarking algorithm for three-dimensional point-cloud models based on vertex curvature, Int. J. Distrib. Sens. Networks 15 (1) (2019) 1550147719826042.
[131] F. Xiaoqing, A watermarking for 3D point cloud model using distance normalization modulation, ICCSNT, in: 2015 4th International Conference on Computer Science and Network Technology, vol. 1, IEEE, 2015, pp. 1449–1452.
[132] J. Liu, Y. Yang, D. Ma, A blind 3d point cloud watermarking algorithm based on azimuth angle modulation, in: 2018 11th International Congress on Image and Signal Processing, BioMedical Engineering and Informatics (CISP-BMEI), IEEE, 2018, pp. 1–7.
[133] K. Bahirat, U. Shah, A.A. Cardenas, B. Prabhakaran, Alert: Adding a secure layer in decision support for advanced driver assistance system (adas), in: Proceedings of the 26th ACM International Conference on Multimedia, 2018, pp. 1984–1992.
[134] Q. Ke, X. Dong-Qing, A self-similarity based robust watermarking scheme for 3D point cloud models, Int. Inf. Inst. (Tokyo). Inf. 16 (6) (2013) 3621.
[135] Z. Zhang, L. Zhang, P. Wang, M. Zhang, T. Tan, Robust watermarking algorithm based on mahalanobis distance and iss feature point for 3D point cloud data, Earth Sci. Informat. 17 (1) (2024) 783–796.
[136] M.C.M.M.M. Marazzi, S. Longari, S. Zanero, Securing LiDAR communication through watermark-based tampering detection, in: Symposium on Vehicles Security and Privacy (VehicleSec), 2024.
[137] F.A. Ferreira, J.B. Lima, A robust 3D point cloud watermarking method based on the graph Fourier transform, Multimedia Tools Appl. 79 (3–4) (2020) 1921–1950.
[138] B. Lipuš, B. Žalik, 3D convex hull-based registration method for point cloud watermark extraction, Sensors 19 (15) (2019) 3268.
[139] M. Zhang, J. Dong, N. Ren, S. Guo, Lossless watermarking algorithm for geographic point cloud data based on vertical stability, ISPRS Int. J. Geo-Information 12 (7) (2023) 294.
[140] Z. Luo, Q. Guo, K.C. Cheung, S. See, R. Wan, CopyRNeRF: Protecting the CopyRight of neural radiance fields, in: Proceedings of the IEEE/CVF International Conference on Computer Vision, 2023, pp. 22401–22411.
[141] C. Li, B.Y. Feng, Z. Fan, P. Pan, Z. Wang, Steganerf: Embedding invisible information within neural radiance fields, in: Proceedings of the IEEE/CVF International Conference on Computer Vision, 2023, pp. 441–453.
[142] L. Chen, J. Liu, Y. Ke, W. Sun, W. Dong, X. Pan, MarkNerf: Watermarking for neural radiance field, 2023, arXiv preprint arXiv:2309.11747.
[143] Y. Jang, D.I. Lee, M. Jang, J.W. Kim, F. Yang, S. Kim, Waterf: Robust watermarks in radiance fields for protection of copyrights, in: Proceedings of the IEEE/CVF Conference on Computer Vision and Pattern Recognition, 2024, pp. 12087–12097.
[144] L. Chen, C. Song, J. Liu, W. Sun, W. Dong, F. Di, IW-nerf: Using implicit watermarks to protect the copyright of neural radiation fields, Appl. Sci. (2076-3417) 14 (14) (2024).
[145] Z. Luo, A. Rocha, B. Shi, Q. Guo, H. Li, R. Wan, The NeRF signature: Codebook-aided watermarking for neural radiance fields, IEEE Trans. Pattern Anal. Mach. Intell. (2025).
[146] X. Zhu, X. Luo, X. Wei, DreaMark: Rooting watermark in score distillation sampling generated neural radiance fields, 2024, arXiv preprint arXiv:2412.15278.
[147] W.K. Ong, K.W. Ng, C.S. Chan, Y.-Z. Song, T. Xiang, Ipr-nerf: Ownership verification meets neural radiance field, 2024.
[148] X. Huang, K.C. Cheung, S. See, R. Wan, Geometrysticker: Enabling ownership claim of recolorized neural radiance fields, in: European Conference on Computer Vision, Springer, 2024, pp. 438–454.
[149] Q. Song, Z. Luo, K.C. Cheung, S. See, R. Wan, Protecting nerfs' copyright via plug-and-play watermarking base model, in: European Conference on Computer Vision, Springer, 2024, pp. 57–73.
[150] W. Sun, J. Liu, W. Dong, L. Chen, F. Di, Rwnerf: Robust watermarking scheme for neural radiance fields based on invertible neural networks., Comput. Mater. Contin. 80 (3) (2024).

[151] M.-S. Kim, R. Prost, H.-Y. Chung, H.-Y. Jung, A blind watermarking for 3-d dynamic mesh model using distribution of temporal wavelet coefficients, in: International Workshop on Multimedia Content Representation, Classification and Security, Springer, 2006, pp. 257–264.
[152] S. Baluja, I. Fischer, Adversarial transformation networks: Learning to generate adversarial examples, 2017, arXiv preprint arXiv:1703.09387.
[153] C.R. Qi, H. Su, K. Mo, L.J. Guibas, Pointnet: Deep learning on point sets for 3d classification and segmentation, in: Proceedings of the IEEE Conference on Computer Vision and Pattern Recognition, 2017, pp. 652–660.
[154] C.R. Qi, L. Yi, H. Su, L.J. Guibas, Pointnet++: Deep hierarchical feature learning on point sets in a metric space, Adv. Neural Inf. Process. Syst. 30 (2017).
[155] A.V. Phan, M.L. Nguyen, Y.L.H. Nguyen, L.T. Bui, DGCNN: A convolutional neural network over large-scale labeled graphs, Neural Netw. 108 (2018) 533–543.
[156] A. Khan, A. Siddiqa, S. Munib, S.A. Malik, A recent survey of reversible watermarking techniques, Inform. Sci. 279 (2014) 251–272.
[157] Q. Zhou, N. Ren, C. Zhu, D. Tong, Storage feature-based watermarking algorithm with coordinate values preservation for vector line data, KSII Trans. Internet Inf. Syst. (TIIS) 12 (7) (2018) 3475–3496.
[158] T. Bhaskar, D. Vasumathi, DCT based watermark embedding into mid frequency of DCT coefficients using luminance component, Int. Res. J. Eng. Technology (IRJET) 2 (3) (2015) 738–741.
[159] S.B.B. Ahmadi, G. Zhang, S. Wei, Robust and hybrid SVD-based image watermarking schemes: A survey, Multimedia Tools Appl. 79 (1) (2020) 1075–1117.
[160] H.S. Malvar, D.A. Florêncio, Improved spread spectrum: A new modulation technique for robust watermarking, IEEE Trans. Signal Process. 51 (4) (2003) 898–905.
[161] K. Wang, G. Lavoué, F. Denis, A. Baskurt, X. He, A benchmark for 3D mesh watermarking, in: Proc. of the IEEE International Conference on Shape Modeling and Applications, 2010, pp. 231–235.
[162] Stanford: The Stanford 3D Scanning Repository, 2023, https://graphics.stanford.edu/data/3Dscanrep/. (Accessed 09 November 2023).
[163] Thingiverse, 2023, https://www.thingiverse.com/. (Accessed 09 November 2023).
[164] Large Geometric Models Archive at Georgia Tech, 2023, https://sites.cc.gatech.edu/projects/large_models/. (Accessed 09 November 2023).
[165] S. Choi, Q.-Y. Zhou, S. Miller, V. Koltun, A large dataset of object scans, 2016, ArXiv:1602.02481.
[166] H. Fu, R. Jia, L. Gao, M. Gong, B. Zhao, S. Maybank, D. Tao, 3D-FUTURE: 3D furniture shape with texture, 2020, arXiv preprint arXiv:2009.09633.
[167] T. Wu, J. Zhang, X. Fu, Y. Wang, J. Ren, L. Pan, W. Wu, L. Yang, J. Wang, C. Qian, et al., Omniobject3d: Large-vocabulary 3d object dataset for realistic perception, reconstruction and generation, in: Proceedings of the IEEE/CVF Conference on Computer Vision and Pattern Recognition, 2023, pp. 803–814.
[168] A. Ranjan, T. Bolkart, S. Sanyal, M.J. Black, Generating 3D faces using convolutional mesh autoencoders, in: European Conference on Computer Vision, ECCV, 2018, pp. 725–741.
[169] C. Fehn, K. Schüür, I. Feldmann, P. Kauff, A. Smolic, Distribution of AT-TEST test sequences for EE4 in MPEG 3DAV, in: MPEG Meeting-ISO/IEC JTC1/SC29/WG11, MPEG02/M9219, 2002.
[170] C.L. Zitnick, S.B. Kang, M. Uyttendaele, S. Winder, R. Szeliski, High-quality video view interpolation using a layered representation, ACM Trans. Graph. 23 (3) (2004) 600–608.
[171] E. Cheng, P. Burton, J. Burton, A. Joseski, I. Burnett, RMIT3Dv: Pre-announcement of a creative commons uncompressed HD 3D video database, in: 2012 Fourth International Workshop on Quality of Multimedia Experience, IEEE, 2012, pp. 212–217.
[172] M. Urvoy, M. Barkowsky, R. Cousseau, Y. Koudota, V. Ricorde, P. Le Callet, J. Gutierrez, N. Garcia, NAMA3Ds1-COSPAD1: Subjective video quality assessment database on coding conditions introducing freely available high quality 3D stereoscopic sequences, in: 2012 Fourth International Workshop on Quality of Multimedia Experience, IEEE, 2012, pp. 109–114.
[173] H. Hirschmuller, D. Scharstein, Evaluation of cost functions for stereo matching, in: 2007 IEEE Conference on Computer Vision and Pattern Recognition, IEEE, 2007, pp. 1–8.
[174] X. Liu, Y. Zhang, S. Hu, S. Kwong, C.-C.J. Kuo, Q. Peng, Subjective and objective video quality assessment of 3D synthesized views with texture/depth compression distortion, IEEE Trans. Image Process. 24 (12) (2015) 4847–4861.
[175] Anaglyph video dataset, 2023, https://www.youtube.com/playlist?list=PLuAqFR-aKaxh0ThTiZhJrVDHu1y058Dvj. (Accessed 09 November 2023).
[176] S. Song, S.P. Lichtenberg, J. Xiao, Sun rgb-d: A rgb-d scene understanding benchmark suite, in: Proceedings of the IEEE Conference on Computer Vision and Pattern Recognition, 2015, pp. 567–576.
[177] C. Fehn, Depth-image-based rendering (DIBR), compression, and transmission for a new approach on 3D-TV, in: Stereoscopic Displays and Virtual Reality Systems XI, vol. 5291, SPIE, 2004, pp. 93–104.
[178] B. Mildenhall, P.P. Srinivasan, M. Tancik, J.T. Barron, R. Ramamoorthi, R. Ng, Nerf: Representing scenes as neural radiance fields for view synthesis, Commun. ACM 65 (1) (2021) 99–106.
[179] B. Mildenhall, P.P. Srinivasan, R. Ortiz-Cayon, N.K. Kalantari, R. Ramamoorthi, R. Ng, A. Kar, Local light field fusion: Practical view synthesis with prescriptive sampling guidelines, ACM Trans. Graph. 38 (4) (2019) 1–14.
[180] R. Martin-Brualla, N. Radwan, M.S. Sajjadi, J.T. Barron, A. Dosovitskiy, D. Duckworth, Nerf in the wild: Neural radiance fields for unconstrained photo collections, in: Proceedings of the IEEE/CVF Conference on Computer Vision and Pattern Recognition, 2021, pp. 7210–7219.
[181] F. Principi, S. Berretti, C. Ferrari, N. Otberdout, M. Daoudi, A. Del Bimbo, The florence 4d facial expression dataset, in: 2023 IEEE 17th International Conference on Automatic Face and Gesture Recognition, FG, IEEE, 2023, pp. 1–6.
[182] D. Cudeiro, T. Bolkart, C. Laidlaw, A. Ranjan, M. Black, Capture, learning, and synthesis of 3D speaking styles, in: Proceedings IEEE Conference on Computer Vision and Pattern Recognition, CVPR, 2019, pp. 10101–10111.
[183] Y. Li, T. Harada, Lepard: Learning partial point cloud matching in rigid and deformable scenes, in: Proceedings of the IEEE/CVF Conference on Computer Vision and Pattern Recognition, 2022, pp. 5554–5564.
[184] A. Chatzitofis, L. Saroglou, P. Boutis, P. Drakoulis, N. Zioulis, S. Subramanyam, B. Kevelham, C. Charbonnier, P. Cesar, D. Zarpalas, et al., HUMAN4d: A human-centric multimodal dataset for motions and immersive media, IEEE Access 8 (2020) 176241–176262.
[185] M. Quanjin, M. Rejab, M. Idris, N.M. Kumar, M. Abdullah, G.R. Reddy, Recent 3D and 4D intelligent printing technologies: A comparative review and future perspective, Procedia Comput. Sci. 167 (2020) 1210–1219.
[186] M. Gaata, W. Puech, S. Sadkhan, S. Hasson, No-reference quality metric for watermarked images based on combining of objective metrics using neural network, in: 2012 3rd International Conference on Image Processing Theory, Tools and Applications, IPTA, IEEE, 2012, pp. 229–234.
[187] E. Gul, S. Ozturk, A novel triple recovery information embedding approach for self-embedded digital image watermarking, Multimedia Tools Appl. 79 (2020) 31239–31264.
[188] E. Gul, A.N. Toprak, Contourlet and discrete cosine transform based quality guaranteed robust image watermarking method using artificial bee colony algorithm, Expert Syst. Appl. 212 (2023) 118730.
[189] H. Liu, Y. Chen, G. Shen, C. Guo, Y. Cui, Robust image watermarking based on hybrid transform and position-adaptive selection, Circuits Systems Signal Process. 44 (4) (2025) 2802–2829.
[190] D. Singh, S.K. Singh, S.S. Udmale, An efficient self-embedding fragile watermarking scheme for image authentication with two chances for recovery capability, Multimedia Tools Appl. 82 (1) (2023) 1045–1066.
[191] A. Renklier, S. Öztürk, Image authentication and recovery: Sudoku puzzle and MD5 hash algorithm based self-embedding fragile image watermarking method, Multimedia Tools Appl. (2023) 1–23.
[192] M. Taşyürek, Odrp: a new approach for spatial street sign detection from exif using deep learning-based object detection, distance estimation, rotation and projection system, Vis. Comput. (2023) 1–21.
[193] D.S. Terzi, N. Azginoglu, In-domain transfer learning strategy for tumor detection on brain MRI, Diagnostics 13 (12) (2023) 2110.
[194] W. Yu, Y. Fan, Y. Zhang, X. Wang, F. Yin, Y. Bai, Y.-P. Cao, Y. Shan, Y. Wu, Z. Sun, et al., Nofa: Nerf-based one-shot facial avatar reconstruction, in: ACM SIGGRAPH 2023 Conference Proceedings, 2023, pp. 1–12.
[195] J.-S. Tsai, J.-T. Hsiao, W.-B. Huang, Y.-H. Kuo, Geodesic-based robust blind watermarking method for three-dimensional mesh animation by using mesh segmentation and vertex trajectory, in: 2012 IEEE International Conference on Acoustics, Speech and Signal Processing, ICASSP, IEEE, 2012, pp. 1757–1760.